ELSEVIER

J. Non-Newtonian Fluid Mech. 109 (2003) 193–230

Journal of Non-Newtonian Fluid Mechanics

www.elsevier.com/locate/jnnfm

Turbulent flow of non-Newtonian liquids over a backward-facing step Part II. Viscoelastic and shear-thinning liquids

R.J. Poole, M.P. Escudier*

Department of Engineering, Mechanical Engineering, University of Liverpool, Brownlow Hill, Liverpool L69 3GH, UK

Received 12 August 2002; received in revised form 28 October 2002

Abstract

The results are reported of an extensive experimental investigation of turbulent flow of polymeric non-Newtonian liquids (0.01, 0.075, 0.125 and 0.175% polyacrylamide (PAA) solutions) through a plane sudden expansion of expansion ratio $R = 1.43$ and aspect ratio $A = 13.3$. Three water-flows are also reported for comparative purposes. A laser Doppler anemometer was used to measure mean and RMS streamwise velocities, U and u', as well as the transverse mean and RMS velocities, V and v', and the Reynolds shear stress $\overline{uv}$. For the water-flows we highlight the important influence on the reattachment length of the maximum turbulence intensity at separation. The PAA flows exhibit an increased reattachment length compared with the Newtonian situation. The magnitudes of the recirculating velocities and recirculating flowrates are increased for the lowest concentration (0.01% PAA) but decreased for the more viscoelastic high concentration (0.075–0.175% PAA) flows. In all cases these changes are accompanied by large reductions in the transverse turbulent intensity. The correspondingly high degree of turbulence anisotropy is instrumental in generating increased reattachment lengths for the lower concentration flows. The increased levels of viscoelasticity for the higher concentration PAA solutions lead to a reduction of the turbulence intensity at separation and this effect, coupled with the high turbulence anisotropy, plays an important role in increasing the reattachment length.

Keywords: Viscoelastic; Shear-thinning; Turbulent; Backward-facing step

1. Introduction

In Part I of this paper [1], the results were reported of the turbulent flow of a 1.5% Laponite solution (which is thixotropic and shear-thinning but of low elasticity) through the same geometry as in this study. It was found that despite its complex rheology the turbulent flow of Laponite was little different to that of water.

* Corresponding author. Tel.: +44-151-794-4804; fax: +44-151-794-4848.
E-mail address: escudier@liv.ac.uk (M.P. Escudier).

0377-0257/02/$ – see front matter
PII: S0377-0257(02)00168-4

Nomenclature

a	constant in Carreau–Yasuda model
A	aspect ratio w/h
b	constant in power-law variation for normal-stress variation
c	concentration by weight of PAA (%)
d	duct height at inlet (m)
D	downstream duct height (m)
h	step height (m)
m	power-law index in power-law variation for normal-stress variation
n	power-law index
N_1	first normal-stress difference (Pa)
$\dot{Q}_\mathrm{A}$	apparent flowrate determined by numerical integration (m^3/s)
$\dot{Q}_\mathrm{F}$	flowrate from flowmeter (m^3/s)
$\dot{Q}_\mathrm{R}$	apparent recirculating flowrate determined by numerical integration (m^3/s)
R	expansion ratio D/d
Re	Reynolds number ($\equiv rhU_\mathrm{B}/m_\mathrm{SEP}$)
u'_SEP	maximum streamwise turbulence intensity at separation (m/s)
$\overline{uv}$	Reynolds shear stress (m^2/s^2)
u'	streamwise turbulence intensity (m/s)
u'_0	freestream turbulence intensity (m/s)
U	mean streamwise velocity (m/s)
U_B	bulk mean velocity $\dot{Q}_\mathrm{F}/wd$ (m/s)
U_RMAX	maximum recirculating streamwise velocity (m/s)
U_0	freestream velocity (m/s)
v'	transverse turbulence intensity (m/s)
V	mean transverse velocity (m/s)
w	channel width (also duct height upstream of smooth contraction) (m)
x	streamwise distance from expansion (m)
x_R	reattachment length (m)
X_R	non-dimensional reattachment length (x_R/h)
y	transverse distance from downstream duct floor (m)

Greek letters

δ	initial boundary-layer thickness (m)
$\dot{\gamma}$	shear-rate (s^{-1})
μ_CH	Carreau–Yasuda viscosity corresponding to characteristic shear-rate ($\dot{\gamma} = U_\mathrm{B}/h$) (Pa s)
μ_CY	Carreau–Yasuda viscosity (Pa s)
μ_M	measured viscosity (Pa s)
μ_SEP	Carreau–Yasuda viscosity corresponding to shear-rate at inlet (Pa s)
μ_∞	infinite-shear-rate viscosity (Pa s)
μ_0	zero-shear-rate viscosity (Pa s)
τ	shear stress (Pa)

Subscripts	
MAX	maximum
0	freestream

Pak et al. [2] used flow visualisation to investigate the flow of two non-Newtonian liquids through an axisymmetric sudden expansion: viscoelastic polyacrylamide (PAA) solutions (and a purely viscous shear-thinning liquid, Carbopol, discussed in Part I). The reattachment lengths for the polyacrylamide solutions were found to be two to three times longer than those for water. Pak et al. [2] hypothesised that this increase was a consequence of suppressed eddy motions within the shear layer resulting from viscoelastic effects.

The phenomenon of drag reduction that occurs with certain non-Newtonian fluids is thought to be associated primarily with viscoelasticity (particularly through the elongational viscosity) but it is still far from being completely understood [3]. The backward-facing step (although not exhibiting drag reduction as such) provides an opportunity to examine the effect of viscoelasticity on turbulence structure in the absence of wall effects. Hibberd [4] and Hibberd et al. [5] in their investigations of the effects of the addition of very small amounts of polyacrylamide (50 ppm) on the turbulent structure of a free turbulent plane shear layer concluded that although PAA reduced the level of small-scale turbulence this did not lead to a general attenuation of turbulence intensities and shear stresses.

The objective of the present study is to examine the influence shear-thinning and viscoelasticity have on the turbulent reattachment process behind a backward-facing step. Four concentrations of polyacrylamide solutions were chosen to encompass a wide range of non-Newtonian characteristics: a very dilute solution, 0.01%, which produces high levels of drag reduction but is only slightly shear-thinning and exhibits low elasticity; an intermediate concentration, 0.075%, which is both moderately shear-thinning and elastic; two high concentrations, 0.125 and 0.175%, which are highly shear-thinning and highly viscoelastic.

2. Experimental rig

The flow loop used for the present experiments was a modified version of that used by Escudier and Smith [6] for their square-duct investigation. The square duct consisted of ten stainless steel modules each of length 1.2 m with an internal cross-section of side length 80 mm. The double backward-facing step, for which the key dimensions are given in Fig. 1, was installed in a replacement module 9.6 m from the inlet connection. The duct width w throughout is 80 mm, the inlet height d is 28 mm, the step height h is 6 mm and the downstream duct height D is 40 mm. These dimensions produce an expansion ratio $R = D/d = 1.43$ and an aspect ratio $A = w/h = 13.3$. By choosing $R < 1.5$ it was anticipated that the flow would be symmetrical if the Abbott and Kline [7] criterion also applies to non-Newtonian fluid flow. Similarly, a value of $A > 10$ was chosen to satisfy de Brederode and Bradshaw's [8] criterion for minimising end effects and three-dimensionality. The expansion was preceded by a short (53.5 mm in length), smooth contraction (40 mm radius followed by 20 mm radius). The region below $y/h = 0.8$ was inaccessible for the transverse LDA beams and so no transverse turbulence intensities or Reynolds shear stresses could be reported below $y/h = 0.8$. Further details of the experimental arrangement and instrumentation can be found in Part I [1].

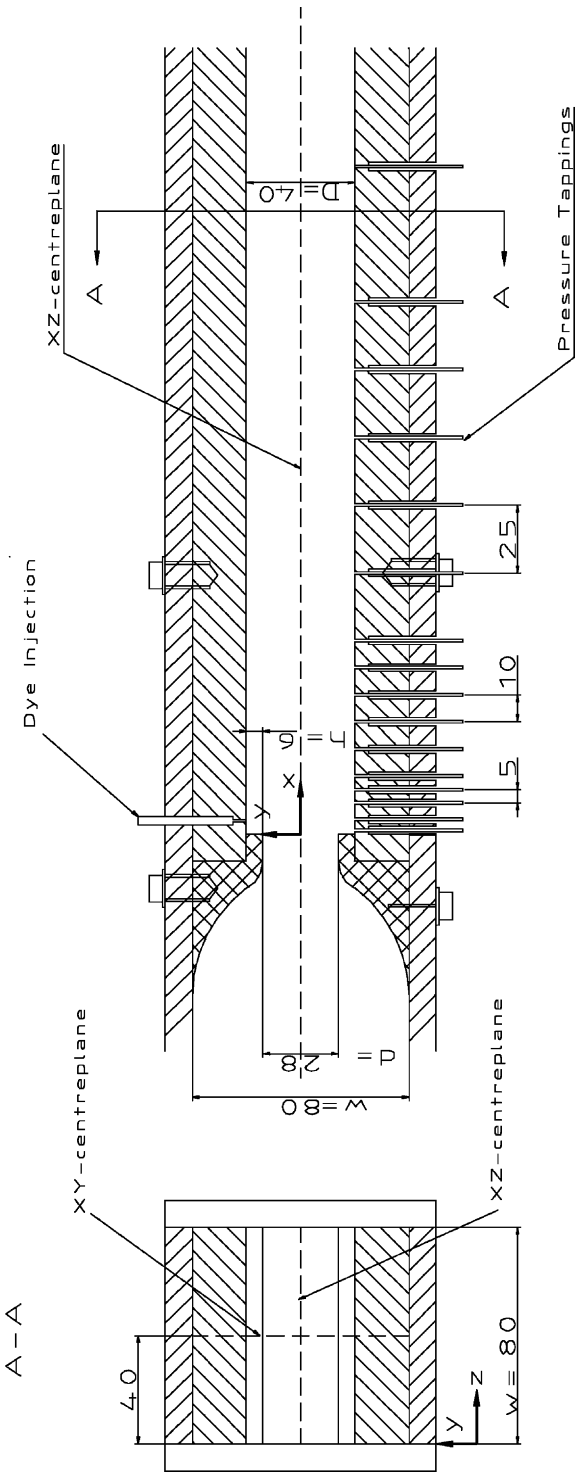

Fig. 1. Backward-facing step geometry, dimensions in millimetres.

3. Rheology of working fluids

The working fluids used in this investigation were various concentrations of aqueous solutions of a polyacrylamide (PAA), Separan AP273 E supplied by SNF UK Limited. The solvent used was filtered tap water with 100 ppm of 40% formaldehyde solution (i.e. 4×10^{-3}% concentration) added to retard bacterial degradation. Approximately 0.25 g of Timiron seeding particles (average size 5 μm) were added to the fluid (total volume of fluid 575 l) to improve the LDA signal quality.

PAA was chosen as the working fluid as it is highly viscoelastic, is optically transparent (thereby permitting LDA measurements) and has been used extensively in previous investigations in the same laboratory (see, e.g. Escudier et al. [3] and Escudier and Smith [6] and elsewhere den Toonder et al. [9] and Stokes et al. [10]). According to Walters et al. [11] PAA is 'very flexible' in its molecular structure and this gives rise to its increased elastic properties compared to other water-soluble polymers such as xanthan gum and carboxymethylcellulose. The average molecular weight for the PAA used in this study, ascertained using gel-phase chromatography, was determined to be 1.94×10^6 kg/kmol with a polydispersity of 1.05. The concentrations of PAA chosen were 0.01, 0.075, 0.125 and 0.175 wt.%. The flow curves (i.e. viscosity versus shear-rate) for the various PAA concentrations are shown in Fig. 2 together with the corresponding Carreau–Yasuda model fits:

$$\mu_{\mathrm{CY}} = \mu_\infty + \frac{\mu_0 - \mu_\infty}{[1 + (\lambda_{\mathrm{CY}}\dot{\gamma})^a]^{n/a}}$$

μ_0 being the zero-shear-rate viscosity, μ_∞ the infinite-shear-rate viscosity, λ_{CY} a time constant, n a power-law index and a is a parameter introduced by Yasuda et al. [12]. The model parameters, which are listed in Table 1, were determined using the fitting procedure (in essence minimisation of the standard deviation, $(1 - \mu_{\mathrm{M}}/\mu_{\mathrm{CY}})^2$) outlined in Escudier et al. [13].

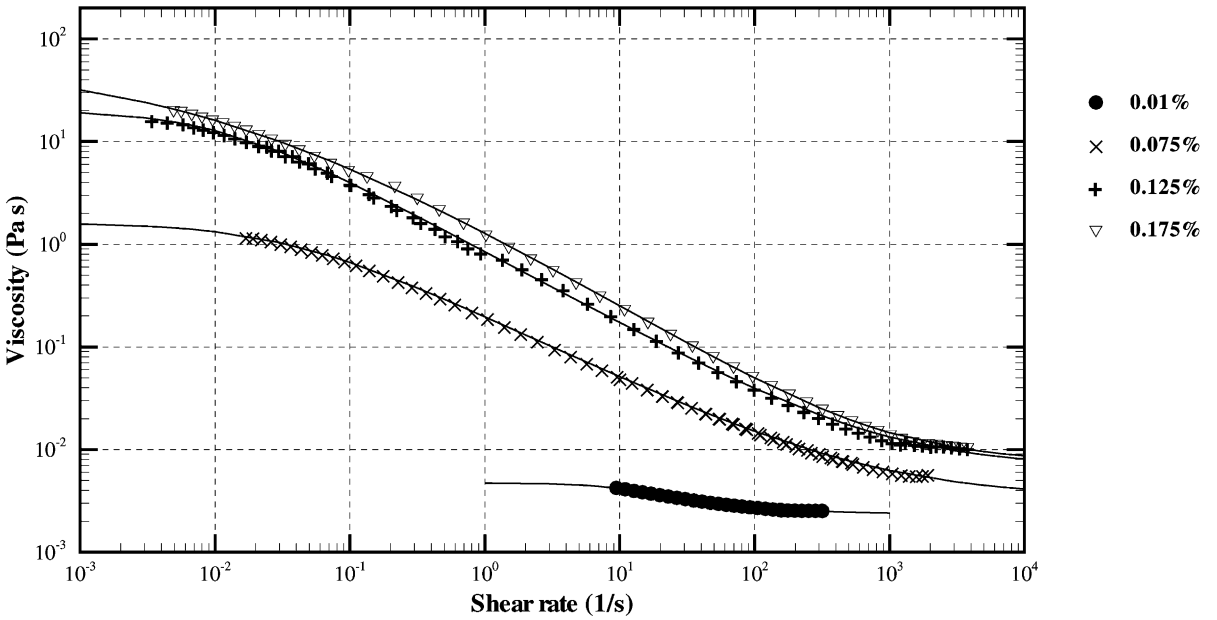

Fig. 2. Viscosity vs. shear-rate for various concentrations of polyacrylamide (including Carreau–Yasuda fits).

Table 1
Carreau–Yasuda model parameters of polyacrylamide

c (%)	μ_0 (Pa s)	μ_∞ (Pa s)	λ_{CY} (s)	n	A
0.01	0.00471	0.00237	0.093	0.858	1.99
0.075	1.62	0.00345	29.9	0.617	0.896
0.125	20.4	0.00682	90.3	0.707	0.978
0.175	58.6	0.00754	89.1	0.790	0.410

The measured variation of the first normal-stress difference N_1, which is a good indicator of the level of elasticity of a fluid versus shear stress, τ, for the three highest concentrations of PAA is shown in Fig. 3. For the lowest concentration (0.01%) the N_1 values produced were below the sensitivity of the rheometer even at the highest shear stresses. The two highest concentrations of PAA, 0.125 and 0.175%, appear to have an N_1 that is practically independent of concentration much as Escudier and Smith [6] observed for high concentrations (0.4–1.5%) of a XG/CMC blend. Power-law fits to the $N_1(\tau)$ data have been included for each fluid in Fig. 3 and the parameters are listed in Table 2.

Although the most dilute solution (i.e. 0.01%) produces a fluid which is only slightly shear-thinning and of very low absolute elasticity, it nevertheless results in very high levels of drag reduction in pipe flow [14]. The 0.075% solution is both moderately shear-thinning (a two-decade reduction in viscosity over a five-decade increase in shear-rate) and highly elastic (based on recoverable shear, $N_1/2\tau$), although not as elastic as the two highest concentrations. The two highest concentrations, 0.125 and 0.175%, have very similar rheological properties: both are highly shear-thinning (a four-decade reduction in viscosity over a seven-decade increase in shear-rate) and highly elastic, the recoverable shear being greater than 0.5 [15].

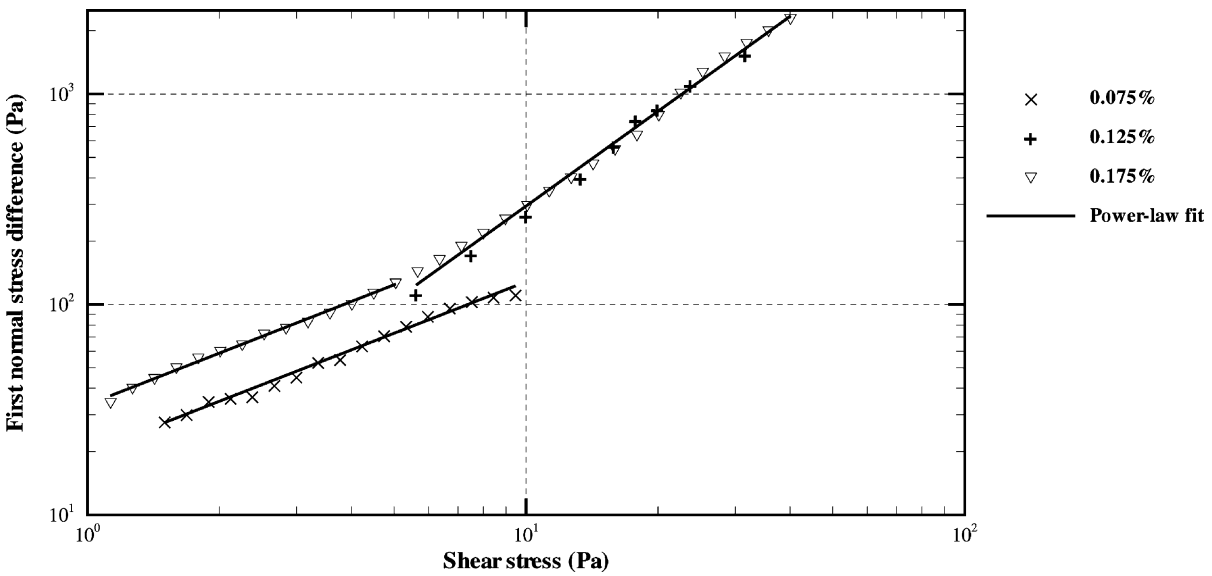

Fig. 3. First normal-stress difference vs. shear stress for various concentrations of polyacrylamide.

Table 2
Power-law parameters for polyacrylamide

c (%)	Range of τ (Pa)	Power-law parameters $N_1 = b\tau^m$	
		b	m
0.075	1.5–10	19.8	0.81
0.125	5.5–40	11.2	1.43
0.175	1–5	33.4	0.81
0.175	5.5–40	11.2	1.43

4. Discussion

4.1. Estimation of Reynolds number

To define a Reynolds number for each flow, we have adopted the step height ($h = 6$ mm) as the appropriate length scale, as is customary in backward-facing step flows [16], the bulk mean velocity (U_B) determined from the flowmeter for the velocity scale and a viscosity estimated from the appropriate flow curve in Fig. 2. corresponding to the shear-rate at the wall at the inlet to the sudden expansion ($x/h = 0$). The density of all the solutions was practically that of the solvent, water. It is also possible to obtain a Reynolds number based on a characteristic viscosity (i.e. the viscosity corresponding to $\dot{\gamma} = U_B/h$) this Re will always be lower than the choice we have adopted and is included in Table 3 for comparative purposes.

4.2. Mean flow

In the interest of clarity the experimental results have been separated into four sections: (A) Newtonian, (B) low concentration (0.01 and 0.075% PAA) and low Reynolds number, (C) low concentration (0.01% PAA) and high Reynolds number, (D) high concentration (0.125 and 0.175% PAA) and low Reynolds number. For each non-Newtonian data set the most appropriate Newtonian data set(s) is (are) included as a basis for comparison. The Newtonian fluid flows are also presented collectively and compared to data from the literature to establish confidence in the experimental apparatus and procedure, and to aid in the non-Newtonian analyses.

Only half profiles are reported since symmetry checks confirmed that each flow was symmetrical about the XZ-centreplane of the duct. To investigate the two-dimensionality of each of the flows, each of the mean streamwise velocity profiles was integrated numerically to estimate an apparent flowrate $\dot{Q}_A$. Fig. 4 shows the comparison between $\dot{Q}_A$ and the flowrate indicated by the flowmeter ($\dot{Q}_F$) for each streamwise location. The figure reveals deviations from two-dimensionality of 5% or less for the water-flows and the low PAA flows. Considering the experimental uncertainty of the results and the numerical technique to estimate the apparent flowrate, it appears reasonable to conclude that these flows are essentially two-dimensional.

For the higher concentrations of PAA deviations much higher than 5% are evident. Upstream of $x/h = 5$ the high concentration PAA $\dot{Q}_A$ is always within 7% of the flowmeter and the majority of values are within 5%. Downstream of this location $\dot{Q}_A$ is up to 22% higher than $\dot{Q}_F$. A clear trend is apparent of increasing apparent flowrate with increasing concentration and downstream distance which suggests that for these flows after reattachment the flow along the centreplane is being accelerated perhaps due to the highly

Table 3
Representative mean flow and turbulence characteristics for a backward-facing step with $h = 6\,\text{mm}$, $D = 40\,\text{mm}$

Fluid	Re ($\equiv \rho U_B h/\mu_{SEP}$)	Re ($\equiv \rho U_B h/\mu_{CH}$)	δ/h	U_B (m/s)	U_0 (m/s)	u'_{SEP}/U_B	u'_0/U_B	U_{RMAX}/U_B	u'_{MAX}/U_B	v'_{MAX}/U_B	$u\bar{v}_{MAX}/U_B^2$	$(\dot{Q}_R/\dot{Q}_A)$ (%)	X_R (x_R/h)
Water	4,000	4,000	0.32	0.664	0.670	0.235	0.0211	−0.220	0.239	0.183	−0.0210	3.46	5.00
Water	14,100	14,100	0.20	2.35	2.36	0.117	0.0234	−0.204	0.223	0.137	−0.0140	3.36	6.33
Water	40,000	40,000	0.15	6.67	6.54	0.09	0.0192	−0.225	0.235	0.153	−0.0176	3.18	6.50
0.01% PAA	4,150	4,050	0.46	1.69	1.74	0.205	0.0120	−0.249	0.241	0.080	−0.0063	3.8	7.67
0.01% PAA	14,700	14,700	0.25	5.92	5.88	0.113	0.0150	−0.340	0.211	0.103	−0.0110	4.9	8.00
0.075% PAA	9,300	6,600	0.50	6.68	7.2	0.145	0.0210	−0.1272	0.229	0.081	−0.0041	1.23	8.33
0.125% PAA	3,800	2,450	0.67	5.54	6.08	0.096	0.0245	−0.0419	0.256	0.085	−0.0087	0.47	8.50
0.175% PAA	4,000	2,850	0.67	6.66	7.27	0.104	0.0218	−0.0459	0.257	0.083	−0.0094	0.40	8.50

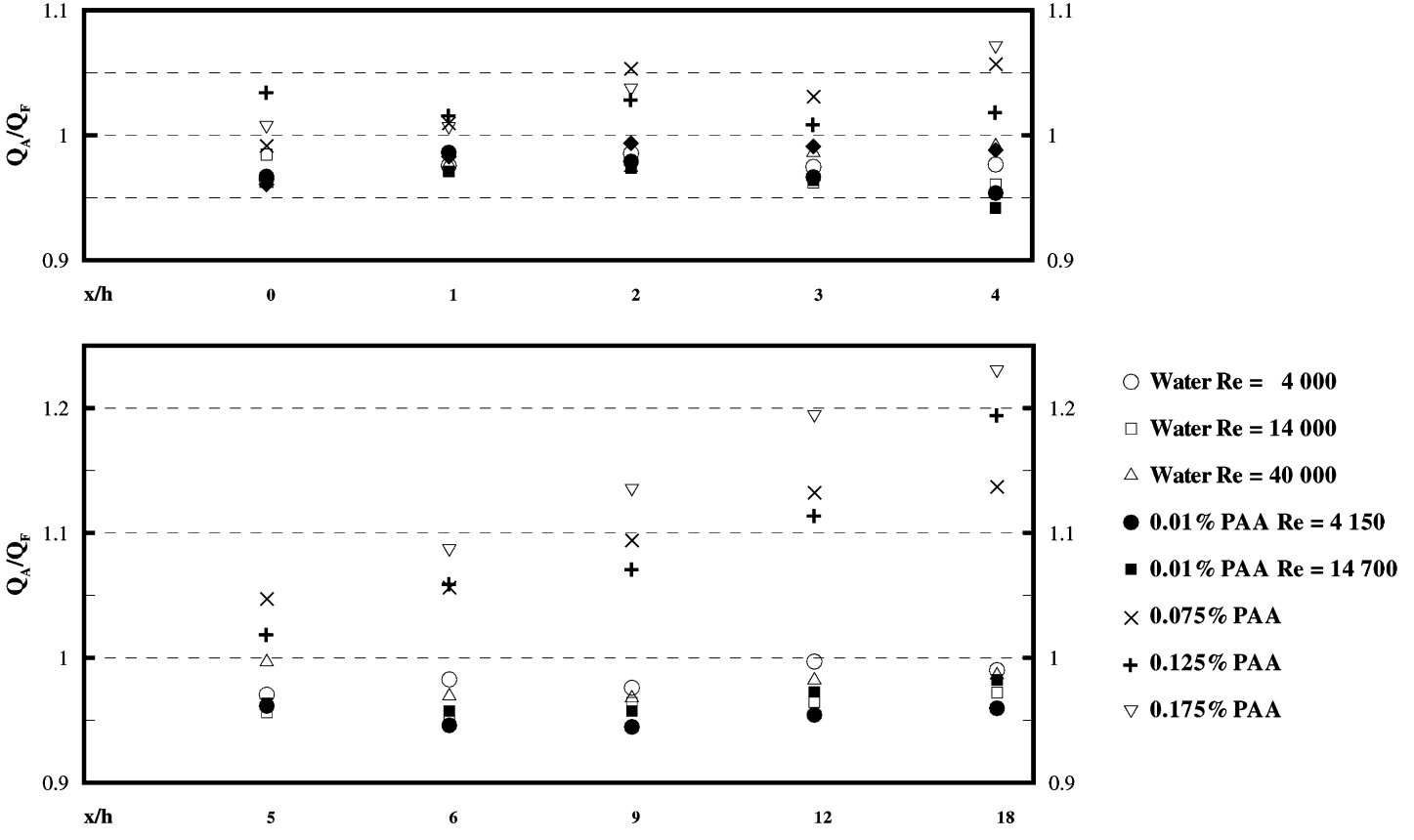

Fig. 4. Comparison between apparent flowrate from integration ($\dot{Q}_A$) and from flowmeter ($\dot{Q}_F$).

viscoelastic nature of the solutions. The associated large normal-stress differences produced would cause the fluid to exert a normal force against the sidewalls of the expansion, which in turn would exert an equal and opposite force on the fluid thus forcing it towards the centreplane. It is clear that for these highly viscoelastic solutions de Brederode and Bradshaw's [8] criterion of aspect ratios greater than 10 producing two-dimensional flows is inapplicable. Even if the aspect ratio were increased it is probable that the nature of the normal-stress difference would still cause the flow along the centreplane to be accelerated.

It is widely accepted [16] that the initial boundary-layer thickness (δ) can have an influence on the flow downstream of a backward-facing step. The magnitude of δ in this study is a direct consequence of the smooth contraction immediately preceding the expansion. At high Reynolds numbers the effect of the contraction is to produce a distribution of velocity at the plane of the expansion which is practically uniform, with a very thin initial boundary-layer ($\delta/h \leq 0.25$) of low turbulence intensity (maximum at the wall $<0.12U_B$). This effect is clearly evident in the higher Reynolds number flows in Fig. 5a and c. For the Newtonian and 0.01% PAA flows at lower Reynolds numbers, δ is larger ($\delta/h < 0.46$) and has a significantly higher near-wall turbulence level at separation from the step ($>0.20U_B$). The higher concentrations of PAA have δ values ($\delta/h < 0.67$) which increase with concentration and reduced levels of turbulence intensity at separation, perhaps a consequence of their viscoelasticity. Adams et al. [17] showed that δ has a relatively weak effect (δ increasing with decreasing X_R) once the Reynolds number is sufficiently high for the boundary-layer to be fully turbulent and, as Isomoto and Honami [18] showed, the reattachment length is much more likely to be sensitive to turbulence intensity levels at separation. However, the differences in δ should be borne in mind during the following discussion.

4.2.1. Newtonian

Fig. 5a shows the mean streamwise velocity (U/U_B) profiles at various downstream streamwise locations for three turbulent water-flows with Reynolds numbers $Re = 4000$, 14,000 and 40,000. All three flows reveal similar mean streamwise velocity profiles. The differences between the two highest *Re* number flows are slight but more substantial for the lowest *Re* number flow and probably attributable to differences either in the boundary-layer thickness at separation or in the inlet turbulence levels. As discussed above, it would seem reasonable to assume that the differences in δ are not responsible for the large difference in reattachment lengths observed for the water-flows (5.0 compared to 6.3/6.5 step heights, see Table 3). A more likely explanation lies in the different levels of near-wall turbulence produced by the smooth contraction at different Reynolds numbers. This question will be addressed in Section 4.3. The reattachment lengths for the water-flows are entirely consistent with values reported previously: in the review by Eaton and Johnston [16] values in the range 4.9–8.2 step heights are reported.

The maximum measured negative velocities within the recirculation region for all three flows are roughly equal to $0.22U_B$ a value in good agreement with previous work: Eaton and Johnston [16] state that the value is 'usually over 20% of the freestream velocity'.

Any differences in the streamwise velocity profiles between the flows diminish downstream of reattachment and by $x/h = 9$ the flows are essentially identical.

The mean flow structure for the water-flows is apparent from the streamline patterns shown in Fig. 6a–c. For all three flows the eye of the recirculation region is located at a streamwise location approximately three step heights upstream of reattachment and half a step height from the wall in the transverse direction. At reattachment, identical values for the non-dimensional streamfunction occur at the same transverse height from the floor of the expansion for all three flows. Table 3 shows that the maximum rates of recirculation ($\dot{Q}_R/\dot{Q}_A$) are approximately equal at about 3.3%.

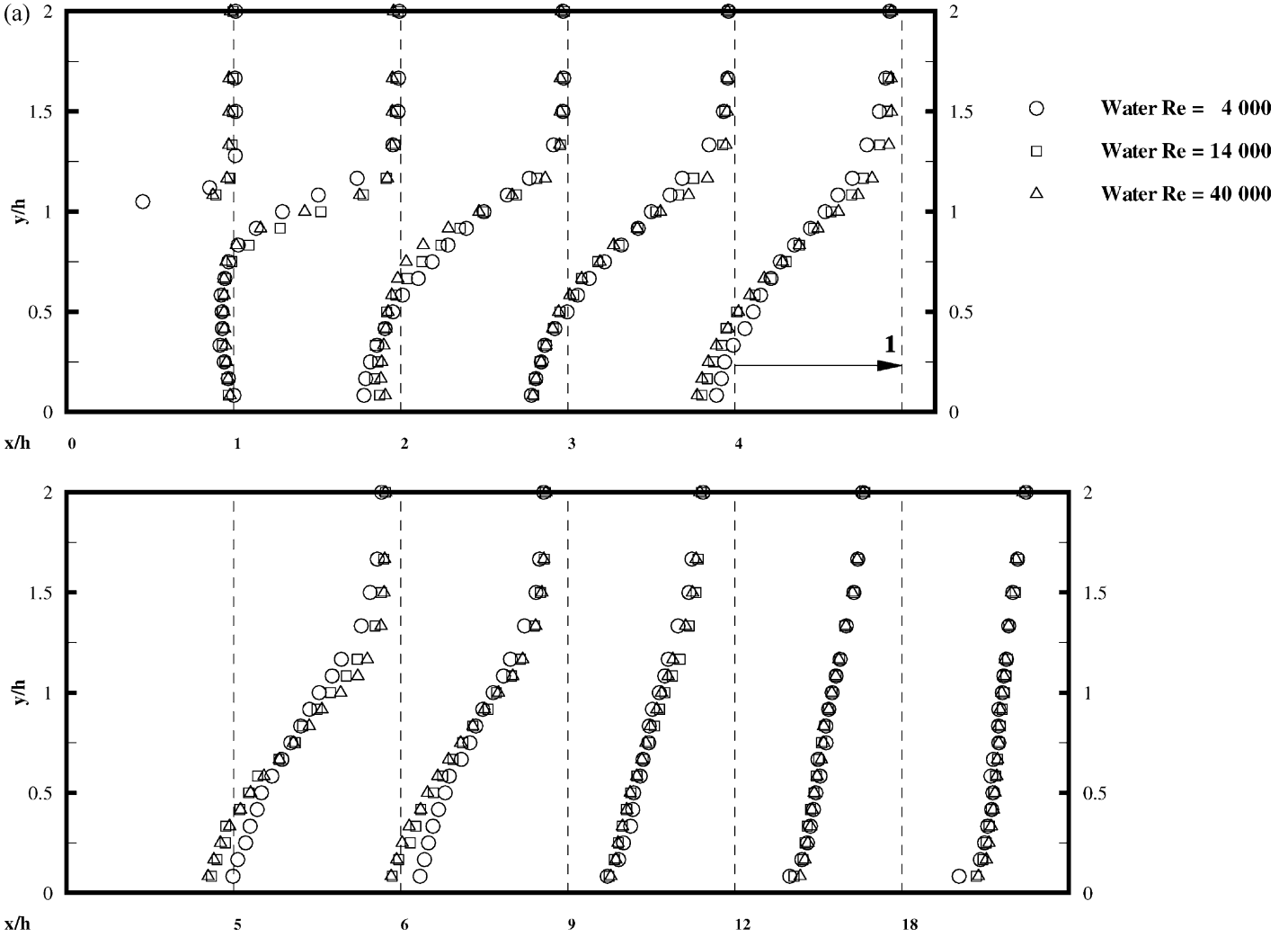

Fig. 5. (a–d) Mean streamwise velocity (U/U_B) profiles.

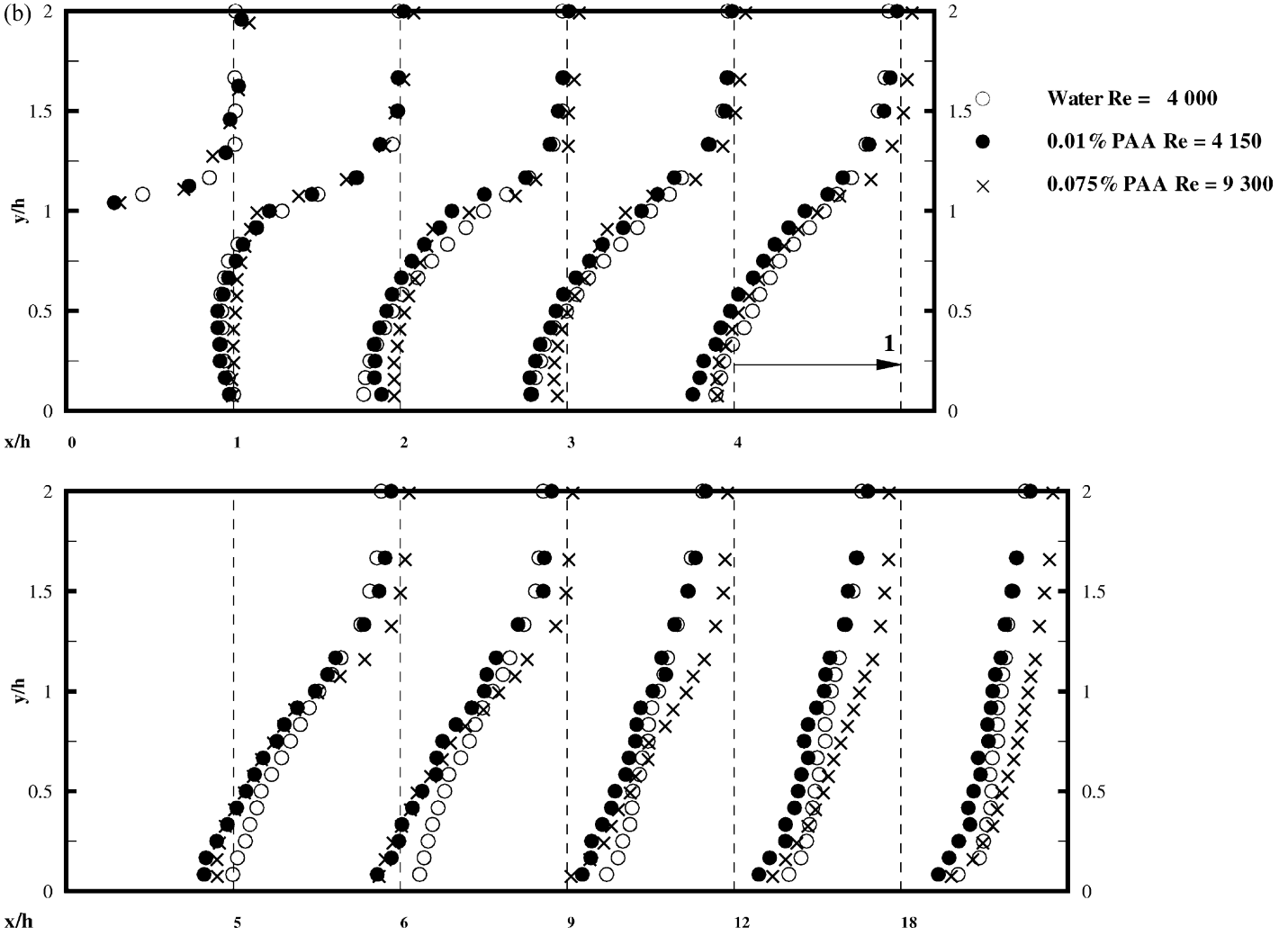

Fig. 5. (*Continued*).

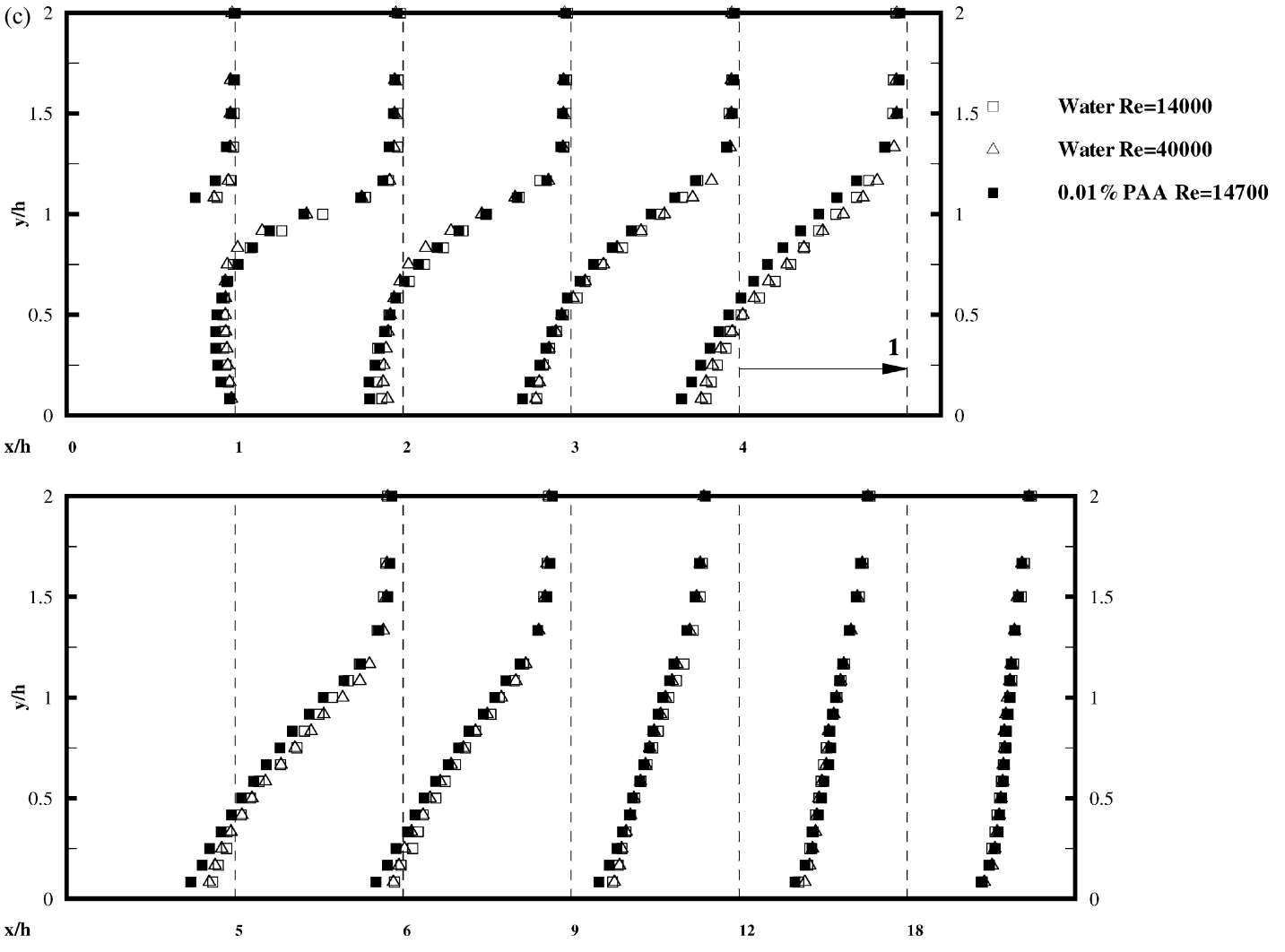

Fig. 5. (*Continued*).

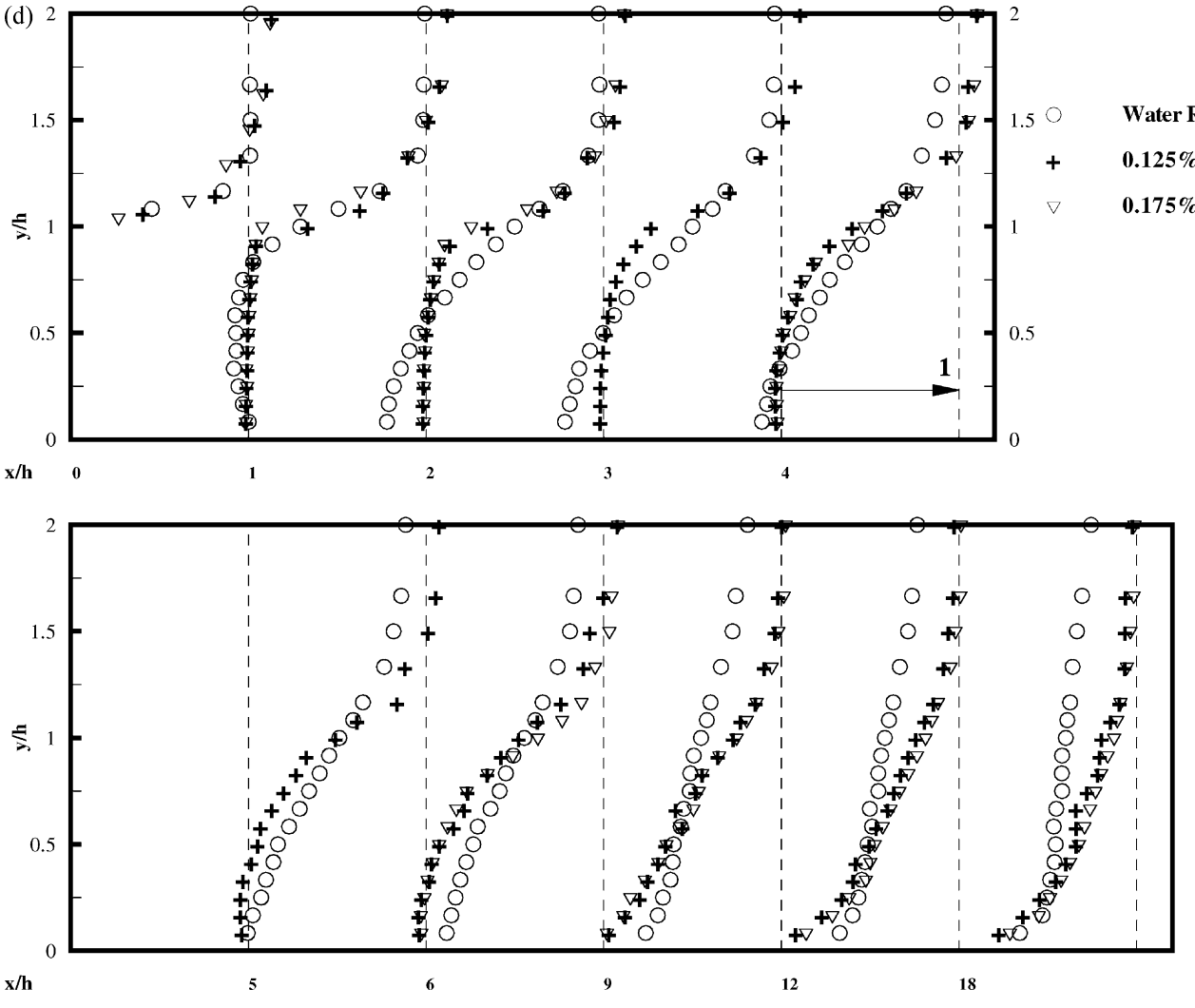

Fig. 5. (*Continued*).

4.2.2. Low concentration (0.01 and 0.075% PAA) and low Reynolds number

Contained within Fig. 5b are the mean streamwise velocity profiles for 0.01% PAA at $Re = 4150$ and for 0.075% PAA at $Re = 9300$. Also shown, for comparative purposes, are the profiles for water at $Re = 4000$. Although both non-Newtonian fluid flows have an increased reattachment length (see Table 3), there are even more fundamental differences compared with the water-flow in their mean flow

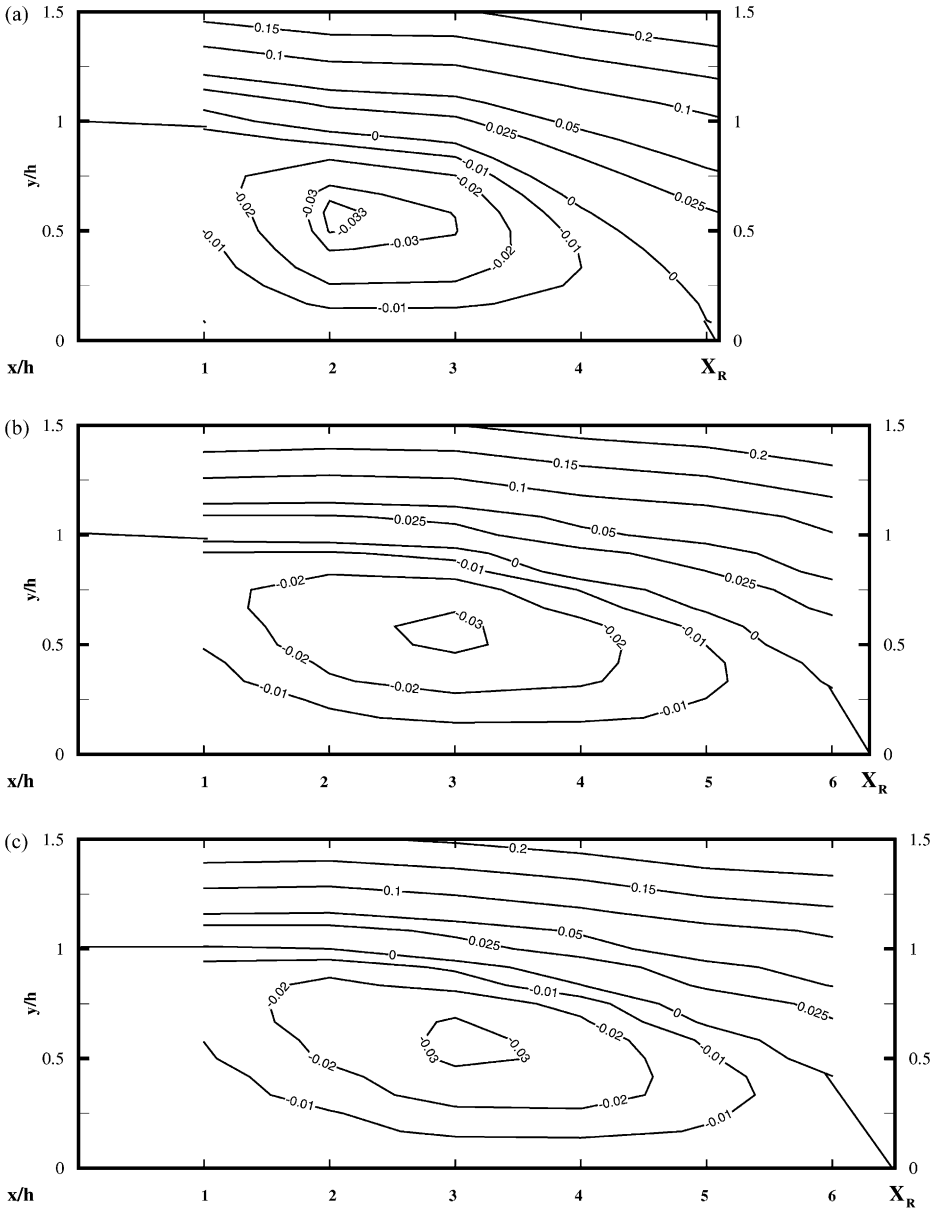

Fig. 6. Streamline patterns: (a) $Re = 4000$ (for water); (b) $Re = 14{,}000$ (for water); (c) $Re = 40{,}000$ (for water); (d) $Re = 4150$ (for 0.01% PAA); (e) $Re = 14{,}700$ (for 0.01% PAA); (f) $Re = 9300$ (for 0.075% PAA); (g) $Re = 3800$ (for 0.125% PAA).

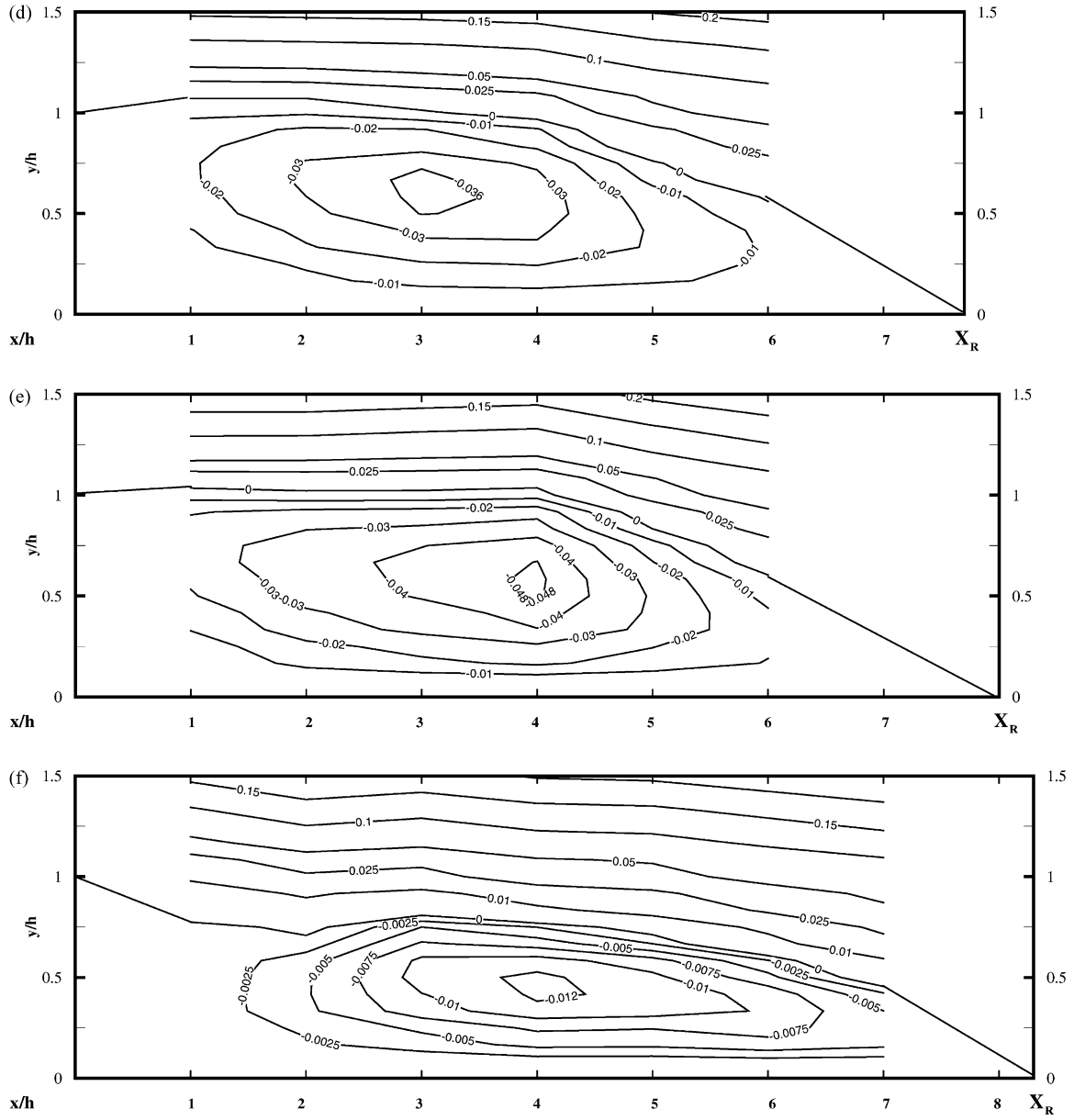

Fig. 6. (*Continued*).

characteristics. The effect of a concentration of PAA as low as 0.01% is significant. The profiles initially are very similar to those for water (at $x/h = 0$ and 1) before major differences become apparent further downstream in the recirculation region. The reattachment length is increased by 50% from 5.0 step heights in the Newtonian case to 7.7 step heights. An increase of about 14% ($0.25U_B$ compared to $0.22U_B$) is also seen in the maximum negative recirculating velocity for the 0.01% PAA flow compared

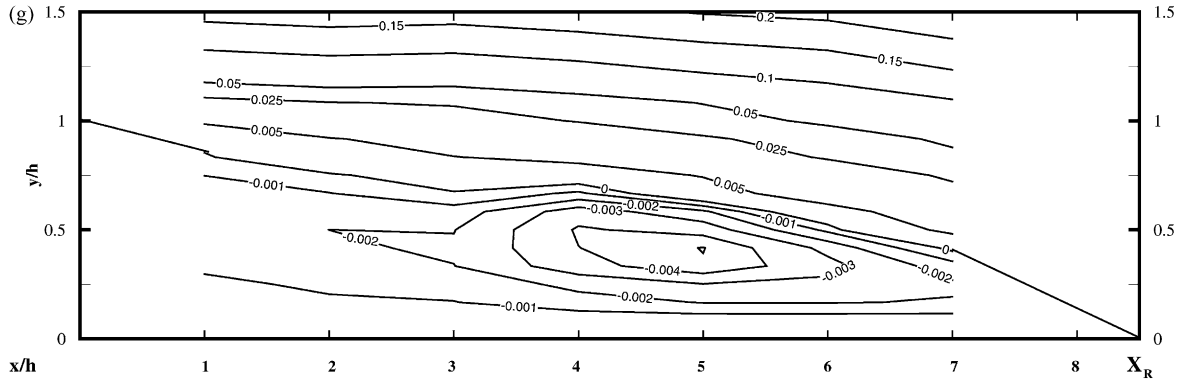

Fig. 6. (*Continued*).

to the water-flow and also in the flowrate of recirculating fluid $\dot{Q}_R/\dot{Q}_A$, from 3.5% for water to 3.8% for PAA. The maximum negative recirculating velocity was detected at the measuring point nearest the wall (0.5 mm) for all flows. For all the water-flows the maximum recirculating negative value was recorded at a streamwise location between two and three step heights upstream of reattachment whereas for the 0.01% PAA $Re = 4150$ it was four step heights.

A further increase in the concentration of PAA (to 0.075%) results in an increased reattachment length (to 8.3 step heights) but other characteristics change in quite a different manner to the low concentration solution: all of the negative velocities are reduced compared to both the water and the 0.01% PAA case, and the maximum negative velocity is reduced by 40% to $0.13U_B$. The recirculating flowrate ($\dot{Q}_R/\dot{Q}_A$) is also decreased significantly, the maximum being reduced from 3.5 to 1.2%.

The streamline patterns for the two PAA solutions shed some light on the different flow structures for these flows. For the 0.01% PAA streamline pattern, shown in Fig. 6d, the increased reattachment length is quite clear with the eye of the recirculation region located further from the reattachment point (>4 step heights) but at the same transverse distance from the wall as for water. As a consequence of the increased reattachment length, upstream of $x/h = 4$ the streamlines in the high-velocity core are essentially straight. The streamline pattern for 0.075% PAA illustrated in Fig. 6f is markedly different. The recirculation region is more compressed transversally with the eye located about 0.4 step heights from the wall and again more than four step heights from the reattachment point in the streamwise direction, in relative terms (based on percentage of reattachment length) this is about the same as the Newtonian high *Re* flows. The reduced level of recirculation is also apparent. At this higher concentration level the PAA rheology appears to result in an expansion of the central high-velocity core thus compressing the recirculation region in the transverse direction and elongating it in the streamwise direction.

4.2.3. Low concentration (0.01% PAA) and high Reynolds number

The mean streamwise velocity profiles for 0.01% PAA at a Reynolds number of 14,700 are shown in Fig. 5c together with the two highest *Re* water-flows. As previously mentioned the initial boundary-layer thickness δ for the non-Newtonian fluid flow is marginally greater than for the two corresponding water-flows. This difference may be caused by the slightly shear-thinning nature of the dilute PAA solution, although the anticipated effect of shear-thinning would be to flatten the profile and hence reduce δ. It may mean that the method of *Re* estimation is too simplistic and that the effective value of *Re* for the

PAA flow is somewhat lower than for the two water-flows. At identical Reynolds numbers this difference in δ is only of the order of $0.05h$ and perhaps the more important parameter is maximum turbulence intensity at separation from the step (see Section 4.3 or [18]) which is approximately equal (to within 3%) for both the non-Newtonian and the water-flow.

As with the earlier discussion, the most noticeable feature brought about by the addition of PAA is an increase in the reattachment length, in this instance by about 25% from 6.3/6.5 to 8 step heights. Also, the PAA flow shows an overall increase in all the negative velocities within the recirculation region compared to the water-flow. The maximum negative recirculating velocity is also increased by over 50%, from $0.22U_B$ to $0.34U_B$ and this is mirrored by an increase in the overall recirculation rate with $\dot{Q}_R/\dot{Q}_A$ increasing by over 50% from 3.2 to 3.4% for the two water-flows to 4.9% for the 0.01% PAA flow (see Table 3). The streamline pattern for this flow (Fig. 6e) confirms this increase in the recirculation and again exhibits essentially straight streamlines up until $x/h = 4$ as was evident in the low Re 0.01% PAA flow. The eye of the recirculation region is located roughly 3.5 step heights upstream of the reattachment location (again about 0.45–$0.5X_R$) and half a step height from the wall in the transverse direction, much as was observed for the equivalent Newtonian fluid flows (Fig. 6b and c). As was the case with the water-flows the differences in the mean streamwise velocity profiles diminish after reattachment ($x/h > 9$) and at $x/h = 18$ the profiles are identical.

4.2.4. High concentration (0.125 and 0.175% PAA) and low Reynolds number

The mean streamwise velocity profiles for the most concentrated PAA solutions used in this study, 0.125 and 0.175%, are shown in Fig. 5d. Both PAA flows have approximately the same Reynolds number of 4000 and so the most appropriate Newtonian comparator is again the $Re = 4000$ water-flow.

At the inlet δ is increased compared to the water-flow, as has been observed previously (Section 4.2.2), in proportion to concentration. Immediately after the expansion, at $x/h = 1$, the 0.175% PAA solution has a narrower shear layer than the 0.125% solution. Downstream of $x/h = 1$ the two sets of non-Newtonian profiles are very similar and any differences are attributable to experimental uncertainty. The apparent agreement suggests that in this concentration range the mean flow field is insensitive to concentration, when the Reynolds number is matched. This similarity is related to the identical levels of viscoelasticity $N_1(\tau)$ in the two solutions, see Section 3.

The differences in the mean streamwise velocity profiles between the water and the PAA flows are now substantial. The reattachment length is increased still further, in this instance by 70% from 5.0 to 8.5 step heights whereas the maximum flowrate of recirculating fluid ($\dot{Q}_R/\dot{Q}_A$) has decreased significantly from 3.5 to <0.5% (see Table 3).

Below the shear layer the non-Newtonian fluid flows are almost stagnant with a maximum negative velocity of less than $0.05U_B$ compared to the Newtonian value of $0.22U_B$. This aspect of the flow is in stark contrast to the very dilute 0.01% PAA solution which shows an increase in reattachment length, recirculation and recirculating velocities. It appears that although the overall length of reattachment is increased for these higher concentrations the recirculation region is actually being suppressed in terms of the quantity of fluid recirculating and the attenuation of the negative velocities. The data for the 0.075% PAA solution is consistent with this behaviour. At these higher concentration levels the effect of the PAA rheology appears to be an expansion of the central high-velocity core thus compressing the recirculation region in the transverse direction and elongating it in the streamwise direction. One possible explanation for the expansion of the core is that it is due to the elastic stresses in the viscoelastic liquids being free to relax after the expansion. This expansion could also be due to the intense shear-thinning of these

solutions or a consequence of shear-thinning in conjunction with turbulence suppression. The results presented in Part I for 1.5% Laponite, which is strongly shear-thinning (indeed it gels on standing), do not display this expansion of the high-velocity core nor do the results of Escudier and Smith [19] for flow of a shear-thinning and drag-reducing solution of 0.25% xanthan gum through an axisymmetric sudden expansion. We conclude that this behaviour cannot be a consequence of shear-thinning alone and is more likely to be related to shear-thinning in conjunction with turbulence suppression. The streamline pattern for the 0.125% PAA solution, shown in Fig. 6g, helps to illustrate this point with compression of the recirculation region in the transverse direction but an overall increase in its length in the streamwise direction. The reduction in the amount of recirculating fluid is also clearly apparent.

4.3. Turbulence structure

4.3.1. Newtonian

The streamwise turbulence profiles (u'/U_B) are shown for the water-flows in Fig. 7a. As was the case with the mean flow the differences between the two highest *Re* numbers are minimal and are restricted to the early part of the shear layer development ($x/h < 3$) where they stem from the differences in the inlet profiles. At inlet ($x/h = 0$) the maximum recorded streamwise turbulence intensity occurs at the first measuring point from the wall for all three flows. This maximum increases with δ and decreases with *Re*. The differences in this near-wall turbulence intensity value are a consequence of the smooth contraction that precedes the expansion. For the higher Reynolds numbers the contraction leads to a uniform velocity profile with a very thin initial boundary-layer and low turbulence intensity at separation ($<0.12U_B$ for both high *Re* flows). For the lower *Re* flow, where viscosity effects are more important, the contraction produces an inlet profile with a thicker initial boundary-layer and a significantly higher streamwise turbulence intensity near the wall of $0.24U_B$. The freestream turbulence levels for all three flows are approximately equal at $0.02U_B$. The significantly higher near-wall turbulence intensity for the lowest *Re* flow leads to universally higher u'/U_B values for this flow up until four step heights downstream of the expansion. The maximum streamwise turbulence intensity for all three flows is approximately equal at $0.23U_B$.

Fig. 10a demonstrates the development of maximum streamwise turbulence intensity as the different flows progress downstream. Upstream of reattachment the lowest *Re* flow exhibits a plateau of almost constant maximum turbulence level as opposed to the steady increase to a global maximum value just upstream of reattachment for the higher *Re* flows. This difference in the levels of turbulence immediately after the step is related to the much higher inlet turbulence intensity of the lowest *Re* flow (see Table 3). Since the inlet turbulence intensity level for this flow is virtually the same as the maximum value attained downstream of the expansion, it is not surprising that this flow demonstrates different behaviour to the higher *Re* flows which have a much lower inlet intensity at separation. A plateau of constant maximum streamwise intensity is also present in the data of Smyth [20] who had a fully developed velocity profile at inlet with high ($\approx 0.18U_B$) turbulence intensity at separation. Downstream of reattachment the data collapse quite well showing a rapid decay in the maximum streamwise turbulence intensity values as has been seen in numerous previous studies (e.g. [16,20,21]). The near-wall development of the streamwise turbulence intensities (Fig. 11a) is qualitatively similar for all three water-flows. Immediately after the step the near-wall turbulence intensity is low ($<0.08U_B$) but increases as the flows progress downstream until just upstream of reattachment where it levels off. This plateau is between 0.12 and $0.14U_B$ for all three flows.

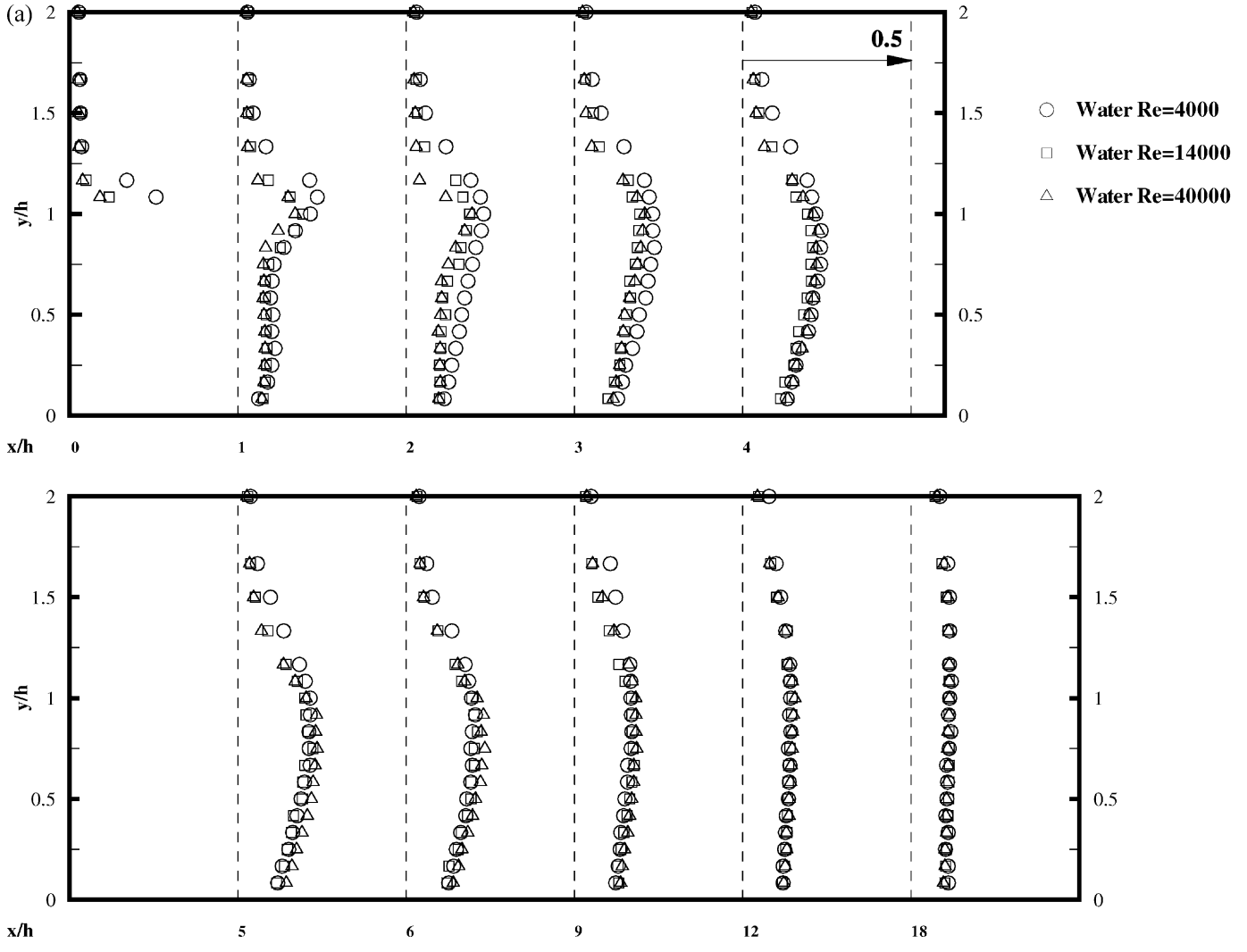

Fig. 7. (a–d) Streamwise turbulence intensity (u'/U_B) profiles.

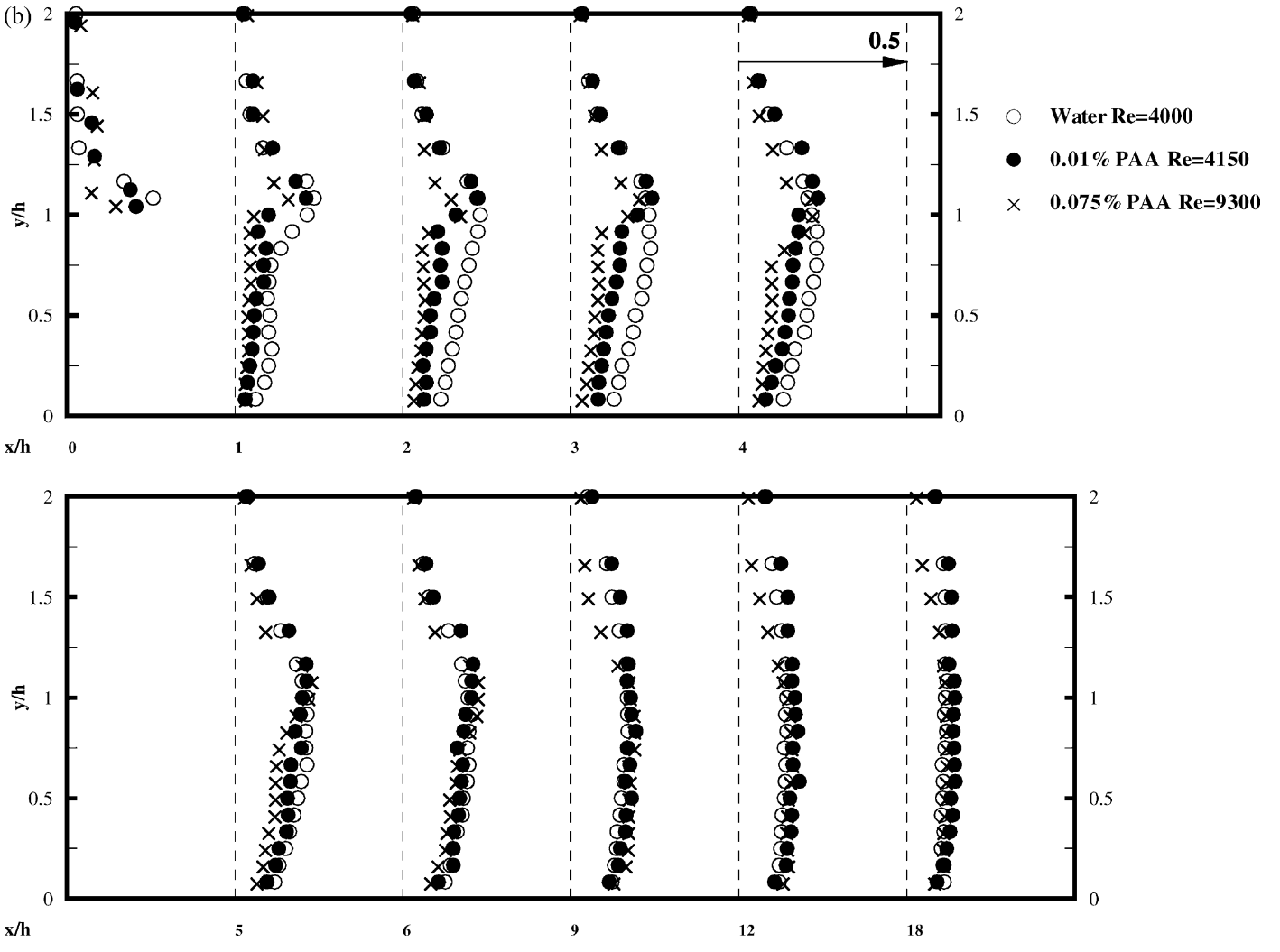

Fig. 7. (*Continued*).

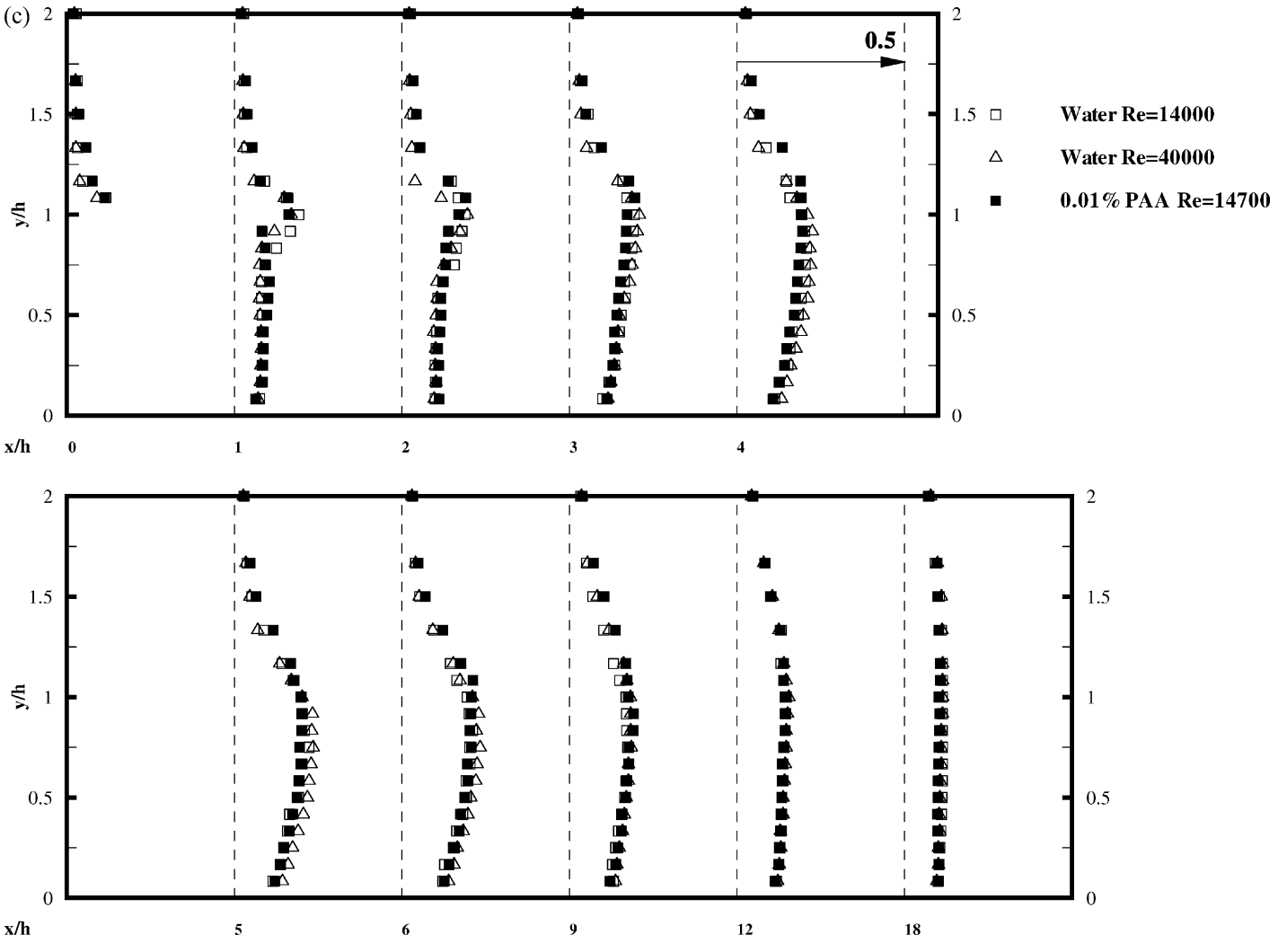

Fig. 7. (*Continued*).

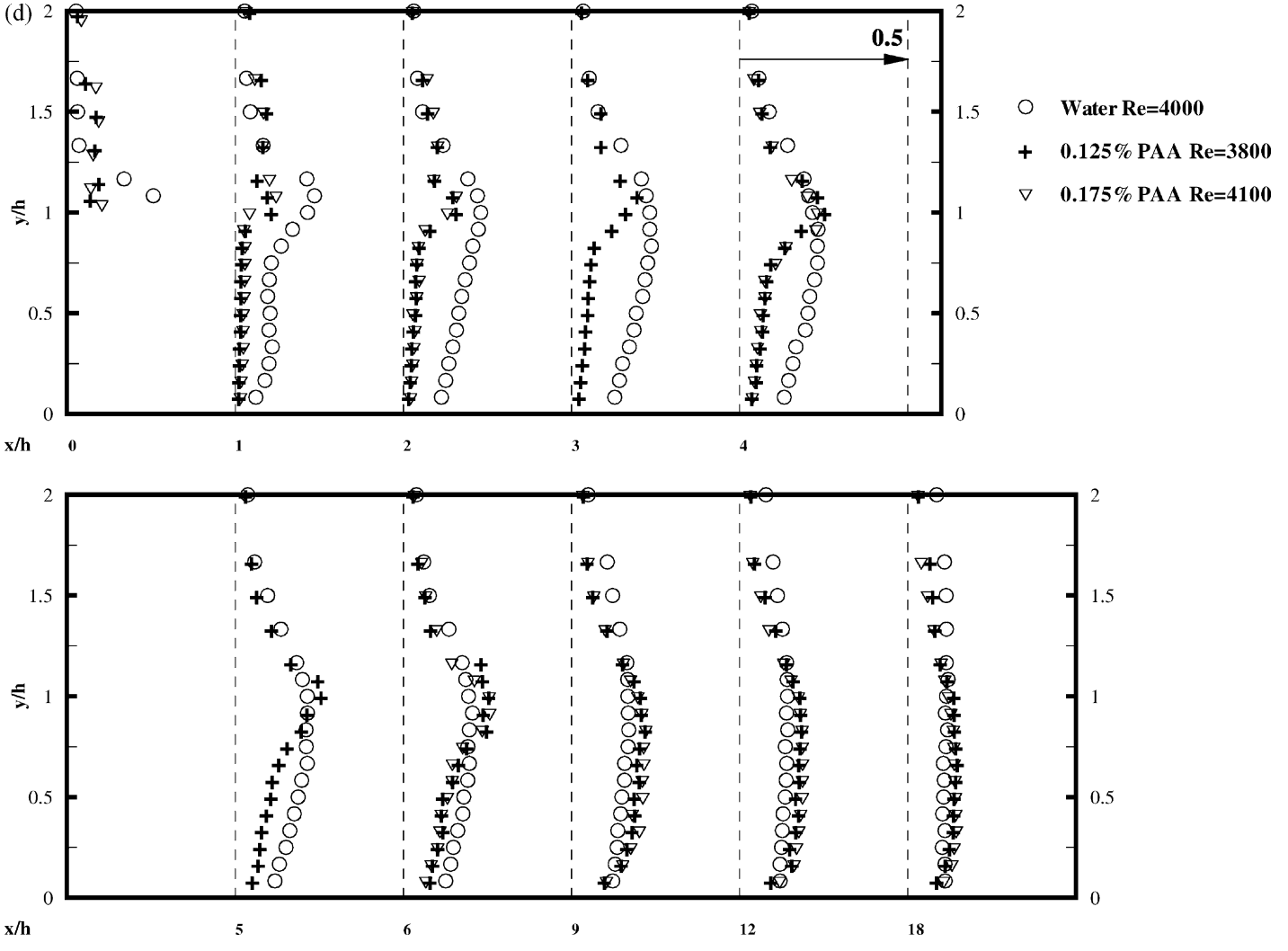

Fig. 7. (*Continued*).

A similar story is presented by the transverse turbulence intensity profiles (Fig. 8a). The transverse turbulence intensity profiles follow the same trajectory as their streamwise counterparts but the peak value is always lower. The turbulence anisotropy is more acute for the two higher *Re* flows where the maximum transverse intensity is considerably lower, 0.14–0.15U_B, than the corresponding streamwise maximum of 0.23U_B, i.e. $u'_{MAX}/v'_{MAX} \approx 1.6$. This anisotropy is not as strong for the lowest *Re* flow where the maximum transverse intensity is 0.18U_B, and upstream of reattachment the transverse intensities for this flow are always higher than for the two other water-flows. The difference in the turbulence structure of the lowest *Re* flow compared to the other two flows is reinforced by the Reynolds shear stress profiles of Fig. 9a: the lower *Re* flow shows greatly increased values of $\overline{uv}$ compared to the other two flows. The $Re = 4000$ flow exhibits markedly different turbulence structure; it has a much larger near-wall turbulence intensity at separation and this leads to a plateau of constant maximum streamwise intensity values immediately downstream of separation, reduced turbulence anisotropy and increased $\overline{uv}$ values. Fig. 12 shows the variation of the maximum Reynolds shear stress with streamwise location and is similar in many aspects to the equivalent streamwise intensity variation (Fig. 10a), the major difference being the much higher maximum values for the lowest *Re* flows.

The difference in turbulence structure between the lowest *Re* flow and the two higher *Re* flows can offer an explanation for the shorter reattachment length of this flow compared to the higher *Re* flows, 5.0 compared to 6.3/6.5 step heights. Isomoto and Honami [18] demonstrated that turbulence intensity at separation has a significant effect on X_R with high values of turbulence intensities at separation leading to shorter reattachment lengths. In the present study, the much higher streamwise turbulence intensity for the lowest *Re* flow leads to a plateau of peak values immediately downstream of the step. Combined with this plateau are greater turbulence isotropy and much higher levels of Reynolds shear stress both of which play important roles in the transport of transverse momentum, leading to a shorter distance to reattachment.

4.3.2. Low concentration (0.01 and 0.075%) and low Reynolds number

The effect of low concentrations of PAA on the streamwise turbulence intensity is shown in Fig. 7b. As we have seen for water, both the mean flow and the turbulent structure are very sensitive to inlet turbulence conditions. For the lowest concentration, 0.01%, the maximum value near the wall is slightly lower than the corresponding water-flow but is still significantly higher than the two high Reynolds number Newtonian fluid flows suggesting that the low *Re* water-flow is still the most appropriate flow with which to compare. The 0.075% PAA solution has a much lower value of streamwise turbulence intensity near the wall at separation. However, as the boundary-layer thickness of this flow is very similar to $Re = 4000$ for both water and 0.01% PAA, this reduction may be related to the increased viscoelasticity of the 0.075% solution.

Downstream of the step there are significant differences in the streamwise turbulence-intensity profiles for the three flows. In the early flow development ($x/h < 5$) on the low-speed side of the shear layer, for the non-Newtonian fluid flows, and particularly for 0.075% PAA, much smaller streamwise turbulence intensities are evident. A number of investigators [16] have commented on the similarities for Newtonian fluids between backward-facing step flow and a plane-mixing layer, although in plane mixing layers the low-speed side of the mixing layer is considerably less turbulent than the high-speed side. The present results suggest that this difference may not occur with non-Newtonian fluids. As the flows progress downstream, up to and beyond reattachment, the low-velocity side of the shear layer becomes more turbulent for the PAA solutions and by $x/h = 6$ the streamwise turbulence intensities are at the same levels as for water-flow.

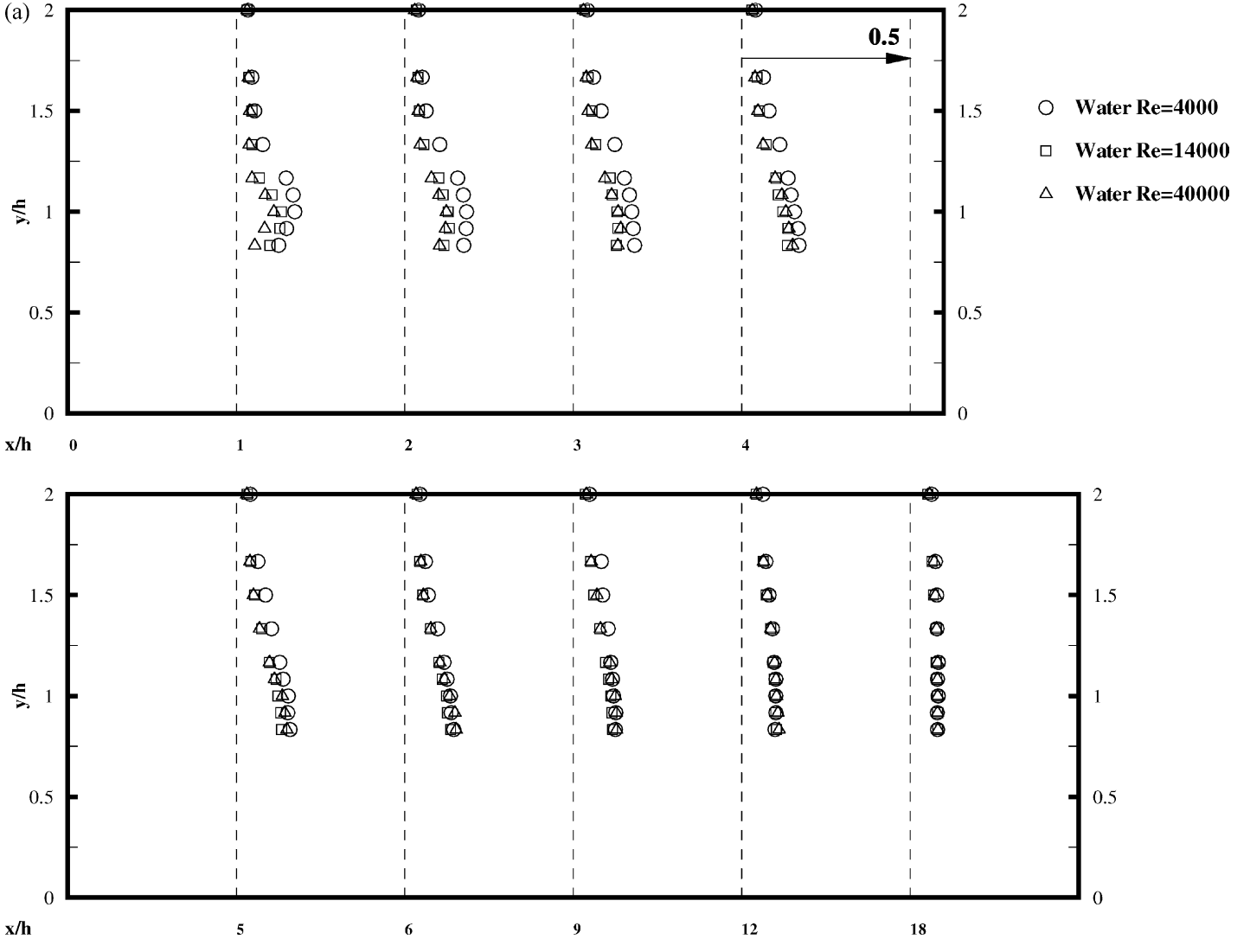

Fig. 8. (a–d) Transverse turbulence intensity (v'/U_B) profiles.

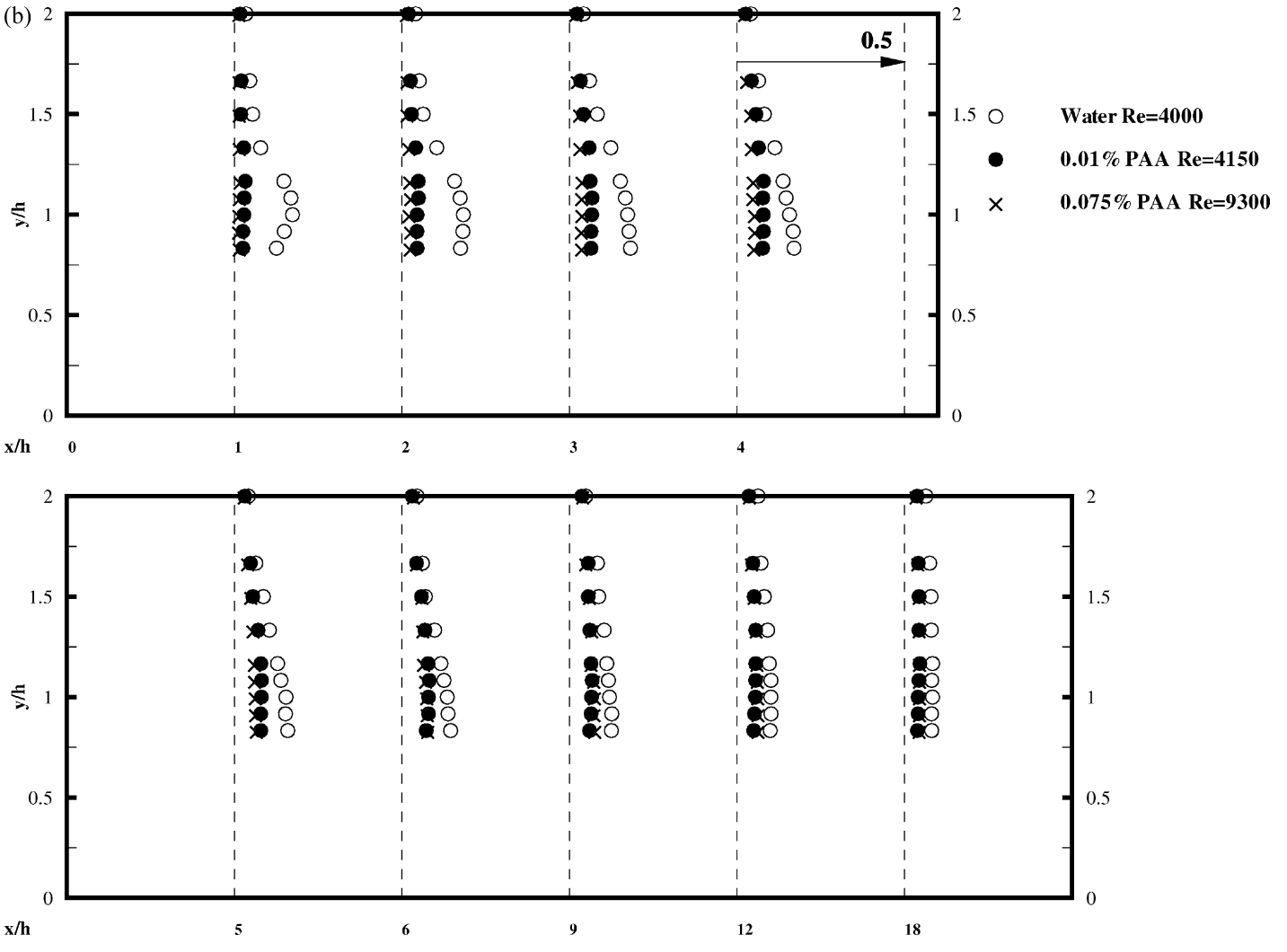

Fig. 8. (*Continued*).

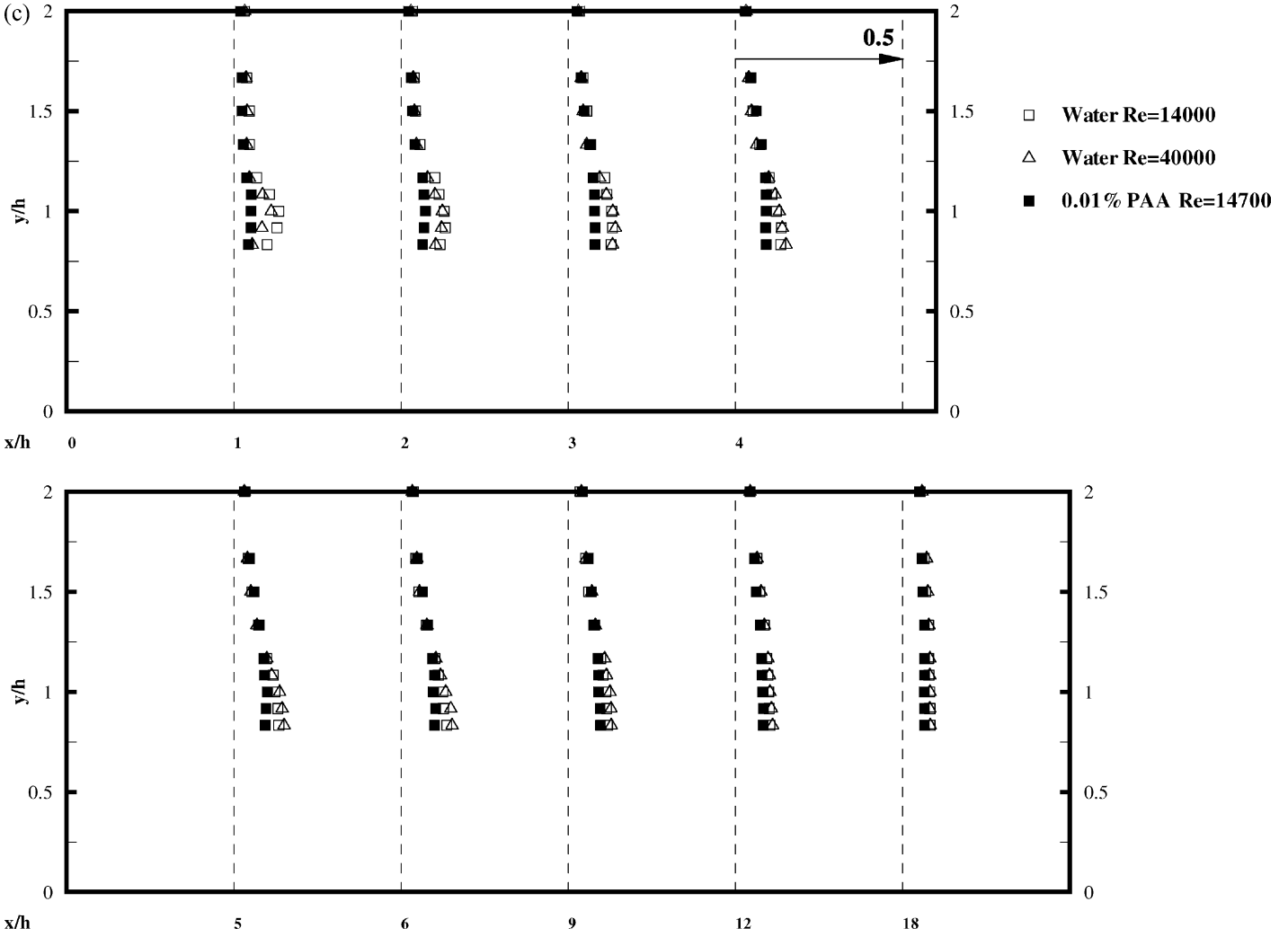

Fig. 8. (*Continued*).

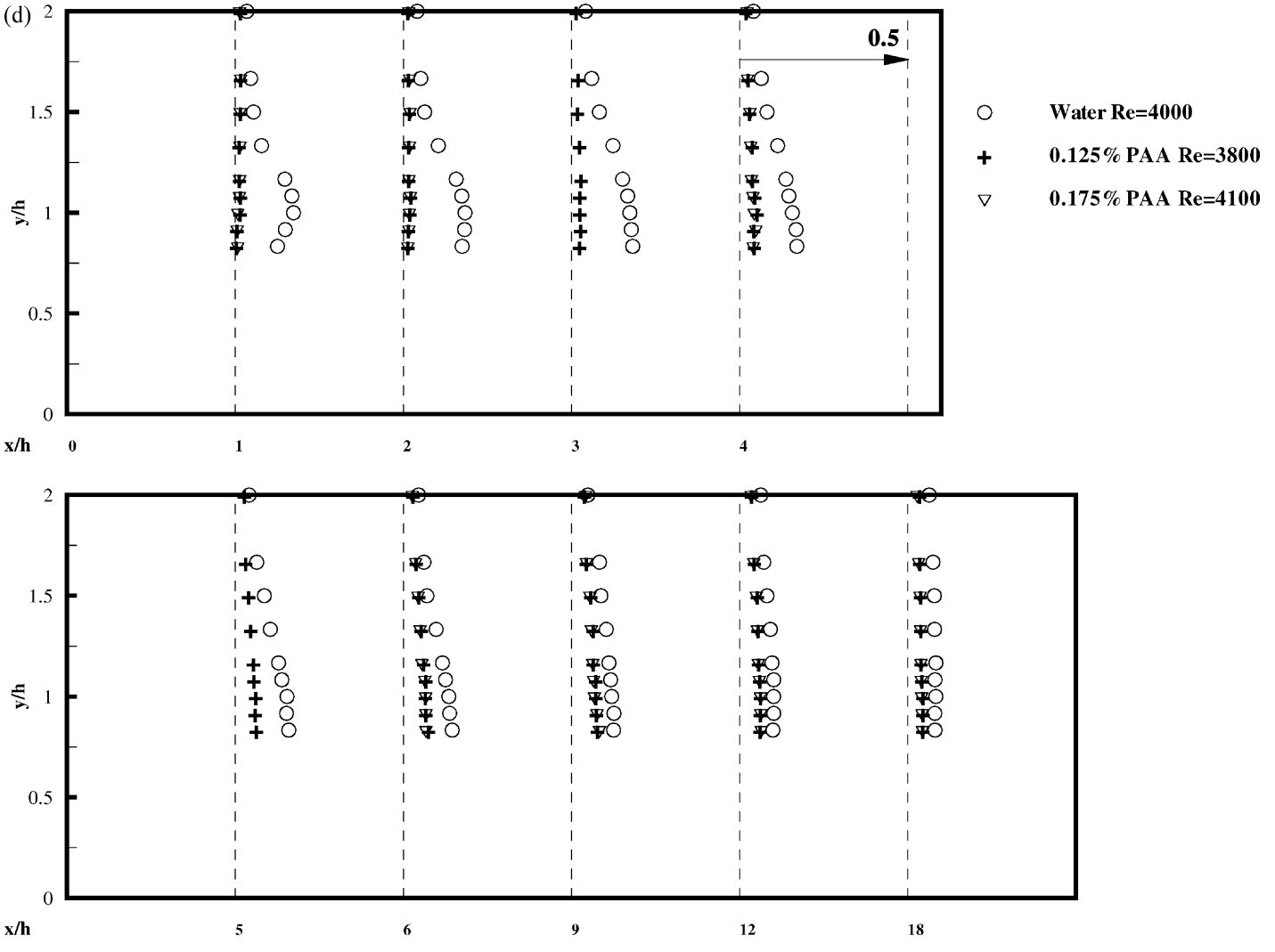

Fig. 8. (*Continued*).

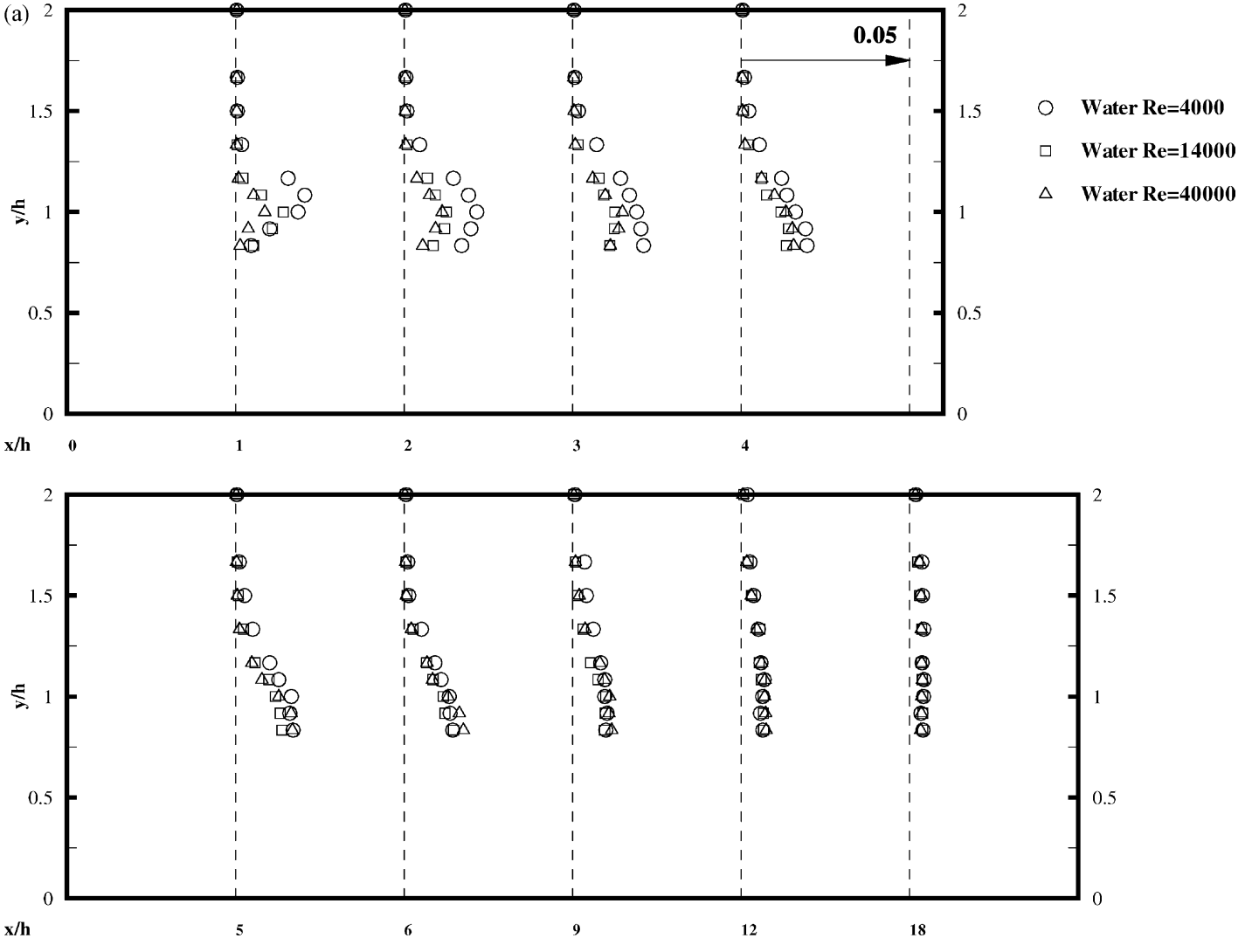

Fig. 9. (a–d) Reynolds shear stress ($\overline{uv}/U_B^2$) profiles.

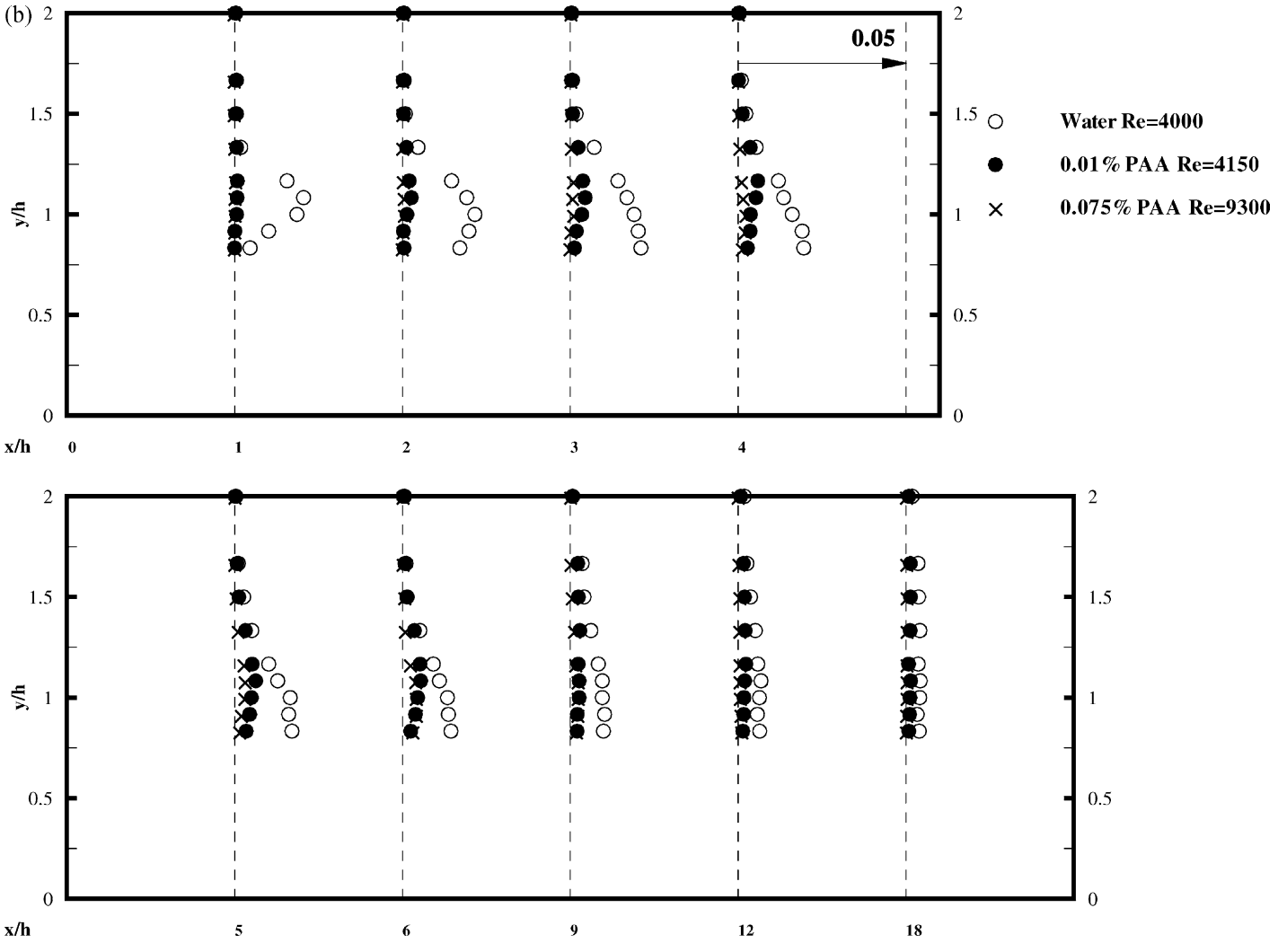

Fig. 9. (*Continued*).

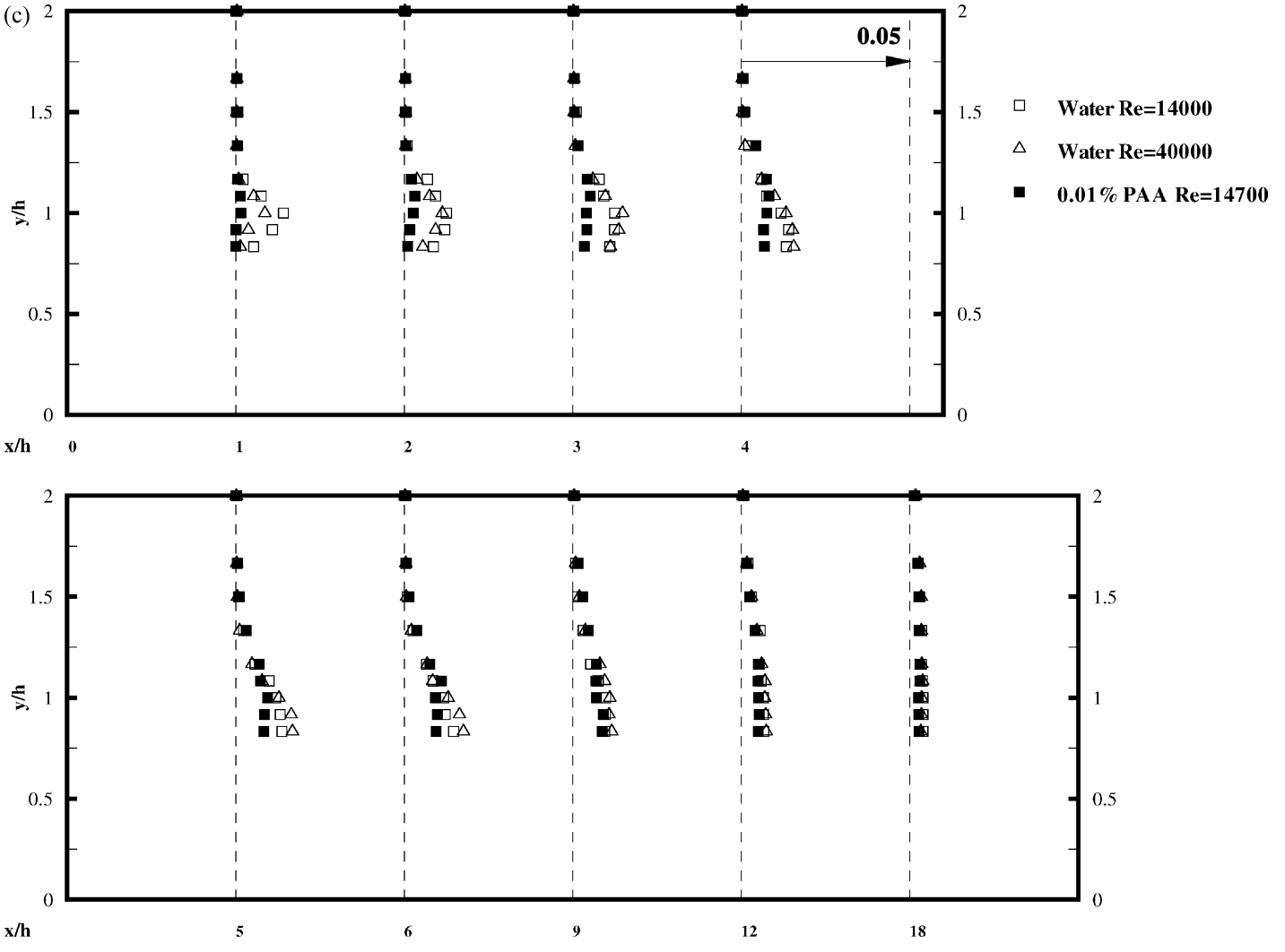

Fig. 9. (*Continued*).

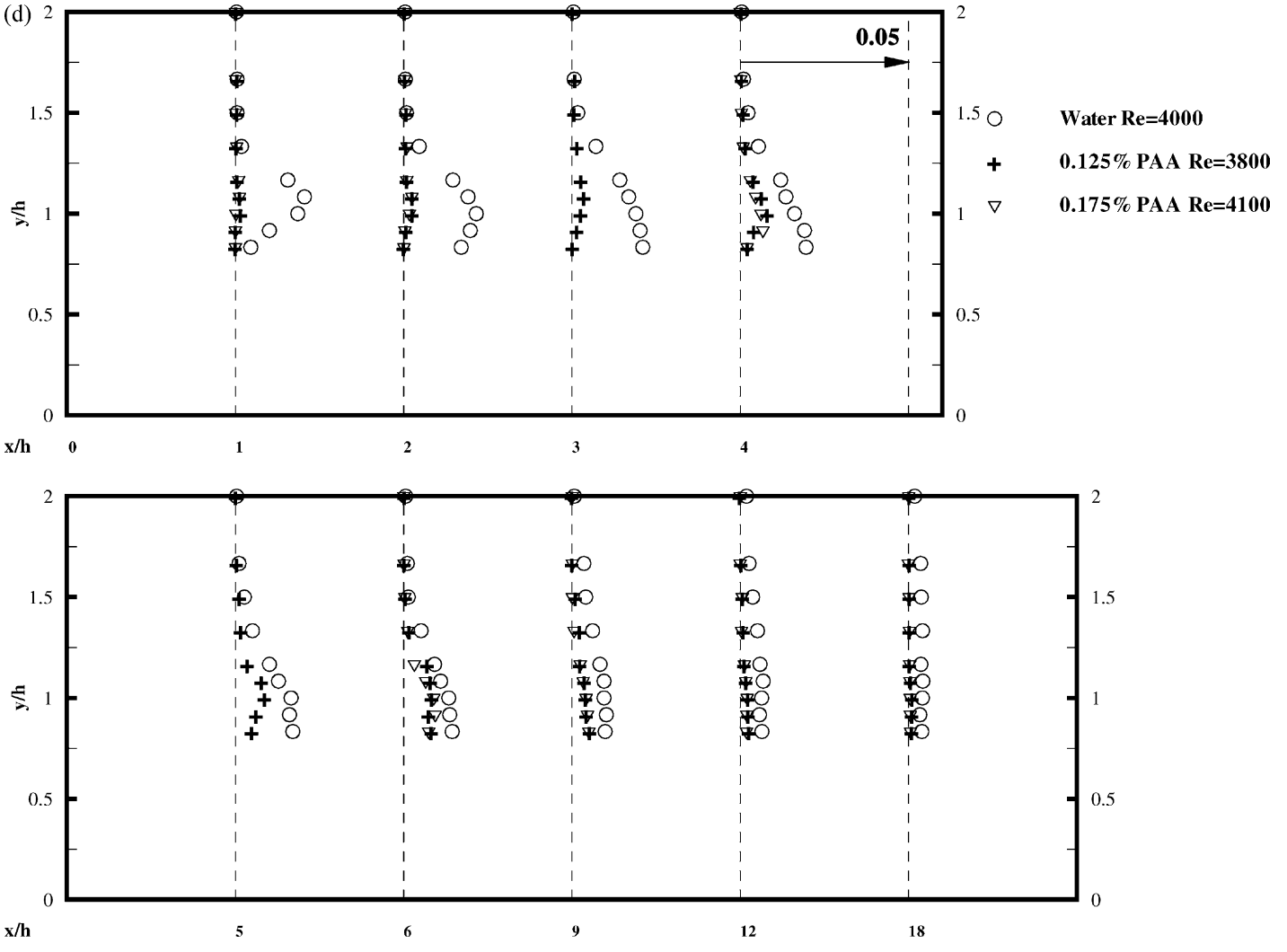

Fig. 9. (*Continued*).

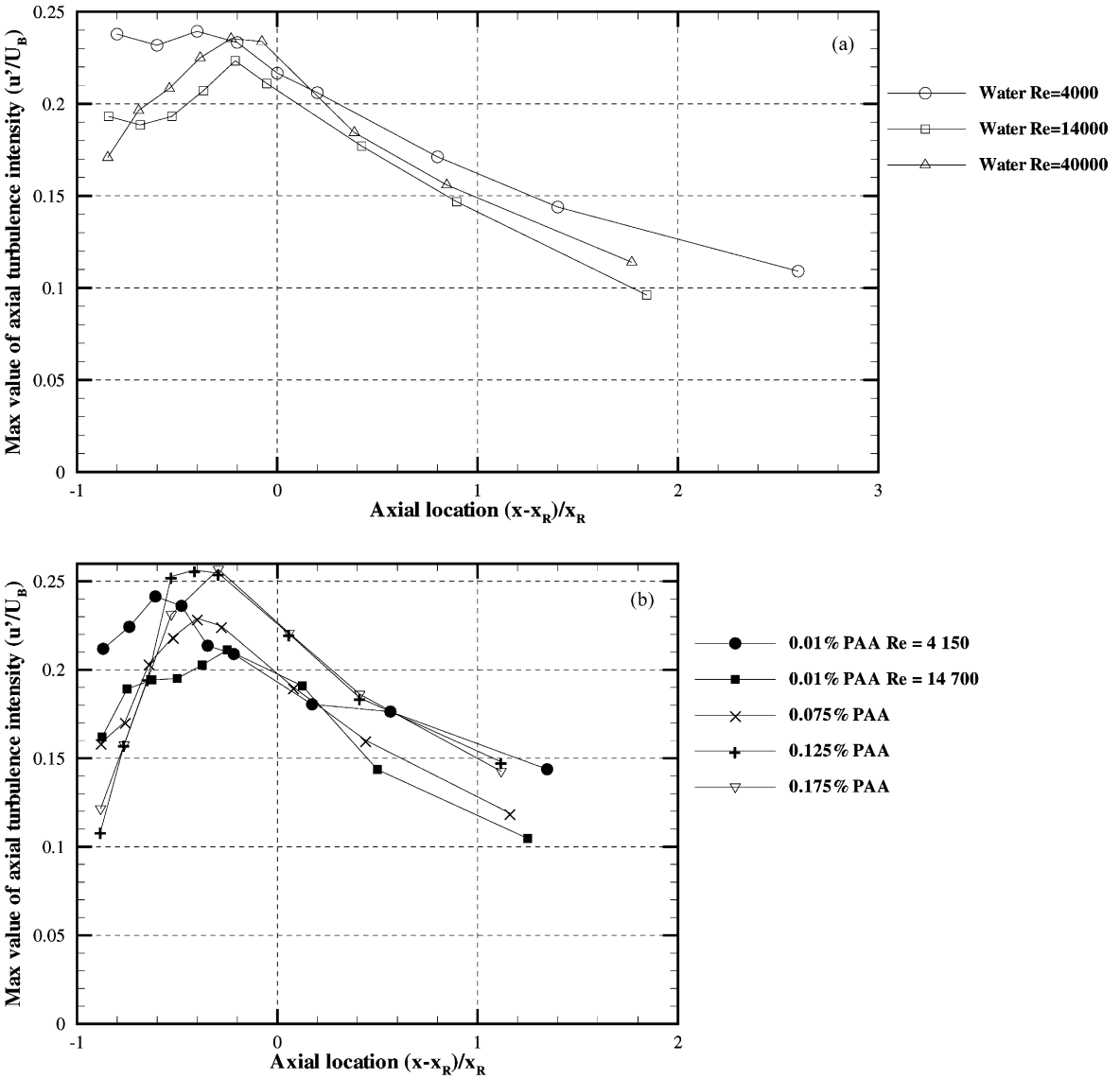

Fig. 10. (a–b) Maximum values of the streamwise turbulence intensity (u'/U_B).

The near-wall variation of u' with streamwise location is shown in Fig. 11b for both non-Newtonian fluid flows and is considerably different from the equivalent water-flow situation (Fig. 11a). Upstream of reattachment the PAA flows exhibit lower values of u' in the near-wall region with the 0.075% concentration showing the greater reduction. Downstream of reattachment the non-Newtonian fluid flows attain a marginally lower plateau level than the equivalent water-flow. The maximum streamwise turbulence intensity is practically identical for the 0.01% PAA flow and the water-flow at $0.24U_B$, but for the 0.075% solution is marginally lower at $0.23U_B$. Despite their different mean and turbulence profiles, the maximum levels of u'/U_B are very similar.

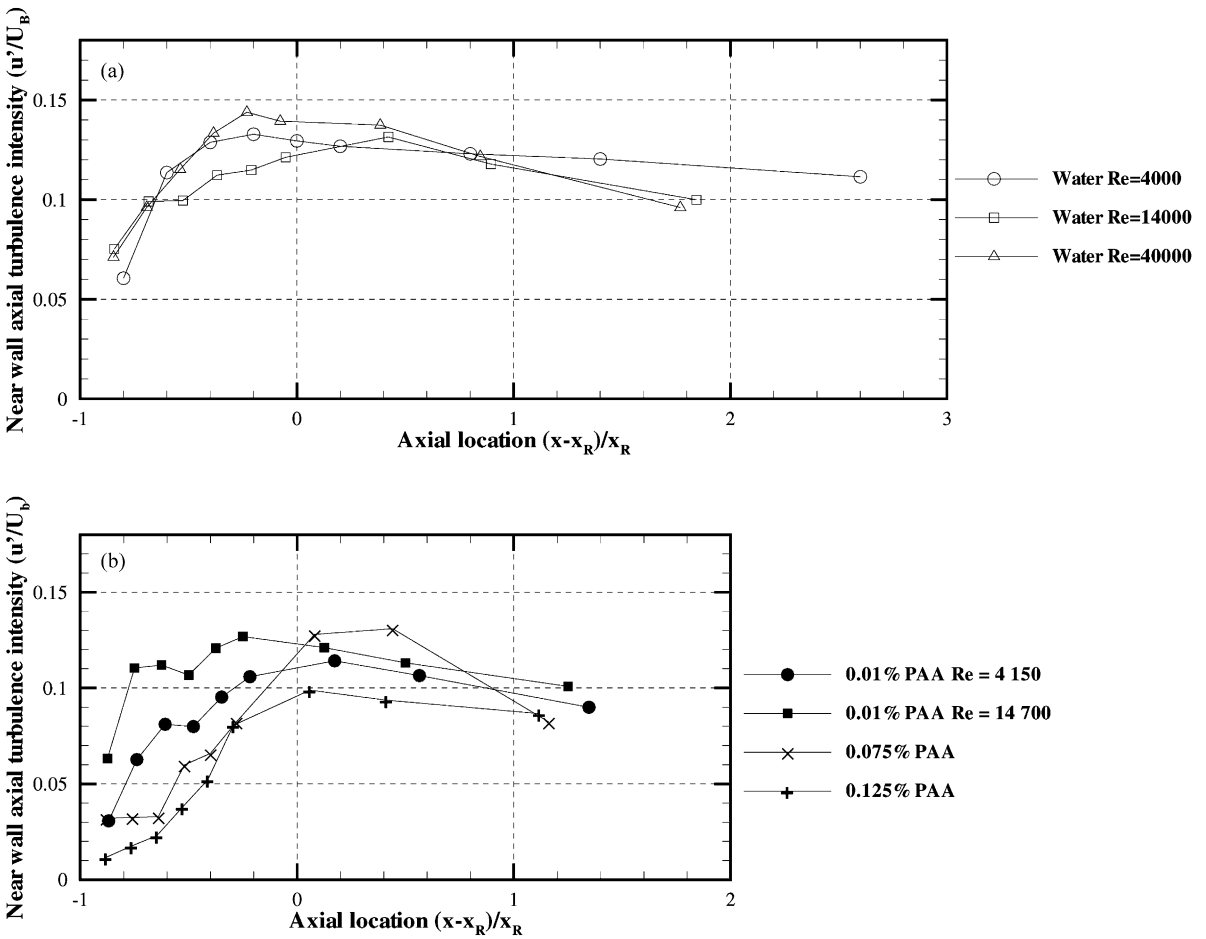

Fig. 11. (a–b) Near-wall values of the streamwise turbulence intensity (u'/U_B).

The differences in transverse intensity are more exaggerated (Fig. 8b). The non-Newtonian fluid flows possess very low levels of transverse intensity with the maximum for both flows only $0.08U_B$. In the early development region ($x/h < 6$), the turbulence anisotropy is higher for the 0.075% concentration but downstream of reattachment the transverse intensity levels are equal for both the PAA solutions and still significantly lower than for water. The non-Newtonian v'/U_B profiles are very flat and do not exhibit the distinct peaks evident in the streamwise turbulence intensities. This high level of anisotropy, with its inevitable lower transport of transverse momentum, must be associated with the longer reattachment lengths for the PAA flows. Such strong anisotropic effects are in keeping with results in the literature for drag reducing non-Newtonian fluids where the turbulence structure is altered (increased streamwise turbulence intensity and decreased transverse turbulence intensity) rather than attenuated [9].

The Reynolds shear stress profiles (Fig. 9b) are more akin to the transverse than the streamwise turbulence intensity profiles. Again the profiles are much flatter than for a Newtonian fluid flow but in this instance have a definite peak located, for both flows, about three and a half step heights upstream of reattachment in the streamwise direction and about one step height above the wall in the transverse

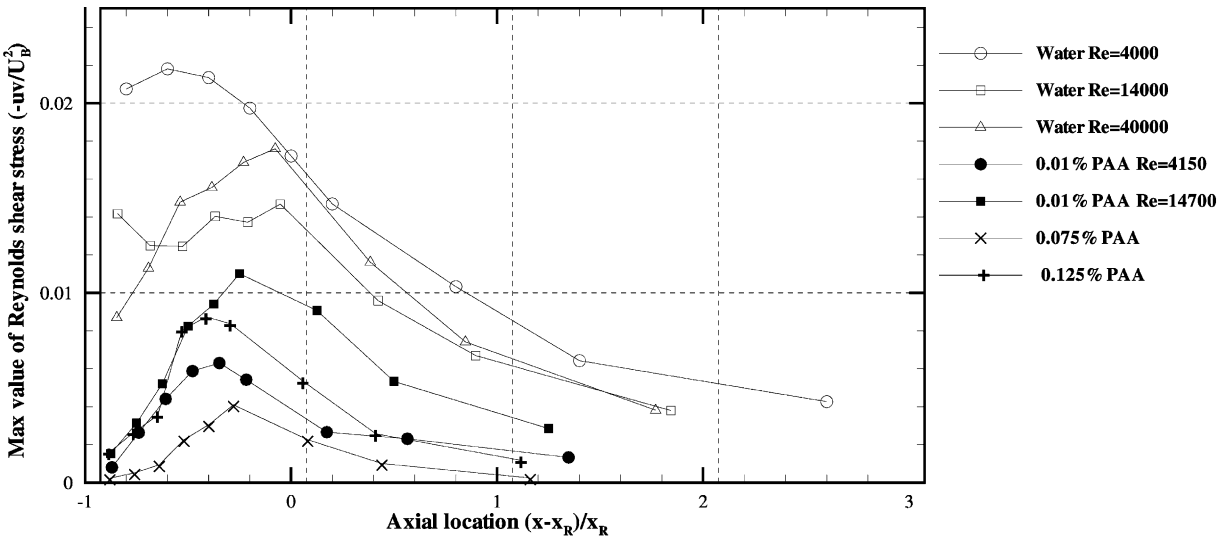

Fig. 12. Maximum values of the Reynolds shear stress ($-\overline{uv}/U_B^2$).

direction. The variation of the local maximum $\overline{uv}$ values (Fig. 12) confirms the much lower values of $\overline{uv}$ for the PAA flows with the local maximum gradually increasing to a global maximum upstream of reattachment before decreasing to very low values ($\overline{uv}/U_B^2 < 0.002$). This behaviour contrasts sharply with the $Re = 4000$ water-flow which has a plateau of high values and a much larger higher maximum.

4.3.3. Low concentration (0.01%) and high Reynolds number

The streamwise turbulence intensity profiles for the low concentration 0.01% PAA at a $Re = 14{,}700$ are presented together with the equivalent water-flow ($Re = 14{,}000$ and 40,000) results in Fig. 7c. The first point of note is at inlet, where the maximum intensity near the wall is identical for the PAA and water-flow at the same Reynolds number (∼14,000).

Despite the significant differences in the mean flow of the 0.01% PAA $Re = 14{,}700$ flow compared to the equivalent water-flow the differences in the streamwise turbulence intensity are small. At $x/h = 1$, the PAA profile is flatter with a narrower region of high turbulence intensity and this increased flatness is apparent throughout the profiles. The development of the local peak streamwise intensity is shown in Fig. 10b and confirms that it is very similar to the corresponding water-flow development. The global maximum is marginally lower, $0.21U_B$, compared to $0.23U_B$ for water, but this may not be representative of the true maximum as the measurements were taken at discrete profile locations and in consequence a difference this small is unlikely to be significant. With this essentially identical streamwise turbulence structure we look to the transverse intensity profiles of Fig. 8c to understand the differences in the mean flow for the 0.01% PAA solution.

The turbulence anisotropy seen in the earlier results for the low *Re* flows of PAA is again evident. The v'/U_B profiles for the PAA flow are much flatter and are always lower in value within the shear layer even at the final measuring location, 18 step heights from the step, and well downstream of reattachment. The maximum value of transverse turbulence intensity is 25% lower than the water-flow for the PAA flow at $0.1U_B$ but is marginally higher than at the lower *Re* where it is $0.08U_B$. The Reynolds shear-stress

profiles for PAA (Fig. 9c) again have more in common with the transverse rather than the streamwise turbulence profiles. They are flatter in shape and display lower values in the shear layer but are identical in the high-velocity core above the shear layer. The maximum value is reduced compared to the value for the water-flow and the percentage reduction is similar to the reduction in the maximum transverse intensity. The streamwise variation of the local maximum Reynolds shear stress is very similar in shape (Fig. 12) to the equivalent water-flow variation but shifted to lower values.

4.3.4. High concentration (0.125 and 0.175% PAA) and low Reynolds number

As the concentration of PAA is increased the effect on the streamwise turbulence intensities (Fig. 7d) is similar to that of the lower concentrations at the same *Re*. At inlet, as was the case with the 0.075% solution, the maximum streamwise turbulence intensity near the wall is reduced significantly (>50%) compared to the low *Re* water-flow. As this effect becomes more pronounced with increasing PAA concentration it seems likely it is related to viscoelasticity. Consequently, the local peak values for the PAA flows are lower in the near vicinity of the step ($x/h < 3$). Fig. 10b shows that the development of the peak values is much more like the higher *Re* water-flows, with a gradual increase downstream of the step, reaching a global maximum just upstream of reattachment. This behaviour is in contrast to the plateau of high streamwise intensity values for the low *Re* water-flow and is a consequence of the reduction in the turbulence intensity at separation.

The maximum streamwise turbulence intensity is slightly accentuated for the PAA flows at $0.26U_B$, an increase of about 10% compared to the Newtonian values. As was the case with the low *Re*, low concentration PAA flows the lower side of the shear layer is much less turbulent than in the water-flows. The near-wall streamwise intensities (Fig. 11b) confirm this trend and also demonstrate that even after reattachment the near-wall values are lower than the water-flow intensities.

There is a tendency for the non-Newtonian profiles to be flatter in shape and for the area of high streamwise turbulence to be narrower than the water-flow profiles. The transverse intensities are shown in Fig. 8d. The profiles are very flat with universally much lower values than the Newtonian equivalent. The levels of turbulence anisotropy are very high, the maximum transverse intensity being only $0.08U_B$, resulting in $u'_{MAX} > 3v'_{MAX}$. The flatness seen in the transverse profiles is again in evidence in the Reynolds shear-stress profiles of Fig. 9d. The maximum Reynolds shear stress is reduced compared to the water-flow but not to the same degree as for the lower concentrations at the same Reynolds number.

5. Concluding remarks

The differences seen in the mean flow of water are related to the different levels of maximum streamwise turbulence intensity at separation. The near-wall u' value for the lowest *Re* flows are much larger and lead to a plateau of high values immediately downstream of the step. Combined with this plateau is lower turbulence anisotropy and much higher Reynolds shear stress resulting in increased transport of transverse momentum and earlier reattachment. The smaller differences in reattachment length for the two higher *Re* flows are in agreement with this mechanism. The maximum recirculating velocity is equal for the three water-flows at about $0.22U_B$, a value consistent with previous investigations.

Very small concentrations of PAA (0.01%) have a surprisingly significant effect on the flow behind a backward-facing step. For both Reynolds numbers studied, an increase in reattachment length was seen with a corresponding increase in the amount of recirculating fluid and in the magnitudes of the

recirculating velocities, with this effect more exaggerated for the higher *Re*. Given the very similar levels of streamwise intensity at separation to the equivalent water-flows, the increase in reattachment length must be attributed to the increased levels of turbulence anisotropy present. The maximum transverse intensity is reduced to less than half of the maximum streamwise intensity and the Reynolds shear stress also shows a marked reduction compared to the water-flow.

As the PAA concentration is increased (0.075–0.125–0.175%) a further increase in reattachment length is observed but with significant mean flow changes compared to both water and the very dilute solutions. The maximum recirculating velocity is reduced as concentration is increased until by 0.175% PAA it is only $0.05U_B$ and the region below the shear layer is almost stagnant. This maximum recirculating velocity is a large reduction from both water-flows ($0.22U_B$) and the 0.01% PAA $Re = 14{,}700$ flow ($0.34U_B$). The quantity of recirculating fluid is also reduced significantly, the effect again becoming more pronounced with increasing concentration. It appears that although at these higher concentration levels the reattachment length is increased, the actual strength of recirculation in terms of velocity magnitude and amount of recirculating fluid is being suppressed. A possible explanation for this suppression is that after the step the elastic stresses stored in the fluid are free to relax and result in an expansion of the high-velocity core, thus compressing the recirculation region in the transverse direction and elongating it in the streamwise. At inlet the effect of viscoelasticity is to reduce the maximum turbulence intensity at separation. This reduction, in conjunction with the increased turbulence anisotropy ($u'_{MAX} > 3v'_{MAX}$) results in the increased reattachment length for these high concentration PAA flows.

Acknowledgements

The authors would like to thank Mr. Mark Flanagan of Unilever Research Port Sunlight for determining the molecular weight of the polyacrylamide used in this study.

References

[1] R.J. Poole, M.P. Escudier, Turbulent flow of non-Newtonian liquids over a backward-facing step. Part I. A thixotropic and shear-thinning liquid, J. Non-Newtonian Fluid Mech. (2002).
[2] B. Pak, Y.I. Cho, S.U. Choi, Separation and reattachment of non-Newtonian fluid flows in a sudden expansion pipe, J. Non-Newtonian Fluid Mech. 37 (1990) 175.
[3] M.P. Escudier, F. Presti, S. Smith, Drag reduction in the turbulent pipe flow of polymers, J. Non-Newtonian Fluid Mech. 81 (1999) 197.
[4] M.F. Hibberd, Influence of polymer additives on turbulence in a mixing layer, in: Essen, B. Gampert (Eds.), Proceedings of the IUTAM Symposium on the Influence of Polymer Additives on Velocity and Temperature Fields, Springer, Berlin, 1985.
[5] M. Hibberd, M. Kwade, R. Scharf, Influence of drag reducing additives on the structure of turbulence in a mixing layer, Rheol. Acta 21 (1982) 582.
[6] M.P. Escudier, S. Smith, Fully developed turbulent flow of non-Newtonian liquids through a square duct, Proc. R. Soc. Lond., Ser. A 457 (2001) 911.
[7] D.E. Abbott, S.J. Kline, Experimental investigation of subsonic turbulent flow over single and double backward facing steps, J. Basic Eng. D84 (1962) 317.
[8] V. de Brederode, P. Bradshaw, Three-dimensional Flow in Nominally Two-dimensional Separation Bubbles. I. Flow Behind a Rearward Facing Step, Aero Report 72-19, Imperial College of Science and Technology, London, UK, 1972.
[9] J.M.J. den Toonder, M.A. Hulsen, G.D.C. Kuiken, F.T.M. Nieuwstadt, Drag reduction by polymer additives in a turbulent pipe flow: numerical and laboratory experiments, J. Fluid Mech. 337 (1997) 193.

[10] J.R. Stokes, L.J.W. Graham, N.J. Lawson, D.V. Boger, Swirling flow of viscoelastic fluids. Part 1. Interaction between inertia and elasticity, J. Fluid Mech. 429 (2001) 67.
[11] K. Walters, A.Q. Bhatti, N. Mori, The influence of polymer conformation on the rheological properties of aqueous polymer solutions, in: D. de Kee, P.N. Kaloni (Eds.), Recent Developments in Structured Continua, vol. 2, Pitman, London, 1990.
[12] K. Yasuda, R.C. Armstrong, R.E. Cohen, Shear flow properties of concentrated solutions of linear and star branched polystyrenes, Rheol. Acta 20 (1981) 163.
[13] M.P. Escudier, I.W. Gouldson, A.S. Pereira, F.T. Pinho, R.J. Poole, On the reproducibility of the rheology of shear-thinning liquids, J. Non-Newtonian Fluid Mech. 97 (2001) 99.
[14] P.S. Virk, Drag reduction fundamentals, AIChE J. 21 (1975) 625.
[15] H.A. Barnes, J.F. Hutton, K. Walters, An Introduction to Rheology, Elsevier, Amsterdam, 1989.
[16] J.K. Eaton, J.P. Johnston, A review of research on subsonic turbulent flow reattachment, AIAA J. 19 (1981) 1093.
[17] E.W. Adams, J.P. Johnston, J.K. Eaton, Experiments on the Structure of Turbulent Reattaching Flow, Report MD-43, Thermosciences Division of the Mechanical Engineering Department, Stanford University, London, UK, 1984.
[18] K. Isomoto, S. Honami, The effect of inlet turbulence intensity on the reattachment process over a backward-facing step, J. Fluids Eng. 111 (1989) 87.
[19] M.P. Escudier, S. Smith, Turbulent flow of Newtonian and shear-thinning liquids through a sudden axisymmetric expansion, Exp. Fluids 27 (1999) 427.
[20] R. Smyth, Turbulent flow over a plane symmetric sudden expansion, J. Fluids Eng. 101 (1979) 348.
[21] E.W. Adams, J.K. Eaton, An LDA study of the backward-facing step flow, including the effects of velocity bias, J. Fluids Eng. 110 (1988) 275.